CANADIAN THESES ON MICROFICHE

I.S.B.N.

THESES CANADIENNES SUR MICROFICHE

National Library of Canada
Collections Development Branch

Canadian Theses on
Microfiche Service

Ottawa, Canada
K1A 0N4

Bibliothèque nationale du Canada
Direction du développement des collections

Service des thèses canadiennes
sur microfiche

NOTICE

The quality of this microfiche is heavily dependent upon the quality of the original thesis submitted for microfilming. Every effort has been made to ensure the highest quality of reproduction possible.

If pages are missing, contact the university which granted the degree.

Some pages may have indistinct print especially if the original pages were typed with a poor typewriter ribbon or if the university sent us a poor photocopy.

Previously copyrighted materials (journal articles, published tests, etc.) are not filmed.

AVIS

La qualité de cette microfiche dépend grandement de la qualité de la thèse soumise au microfilmage. Nous avons tout fait pour assurer une qualité supérieure de reproduction.

S'il manque des pages, veuillez communiquer avec l'université qui a conféré le grade.

La qualité d'impression de certaines pages peut laisser à désirer, surtout si les pages originales ont été dactylographiées à l'aide d'un ruban usé ou si l'université nous a fait parvenir une photocopie de mauvaise qualité.

Les documents qui font déjà l'objet d'un droit d'auteur (articles de revue, examens publiés, etc.) ne sont pas microfilmés.

THIS DISSERTATION
HAS BEEN MICROFILMED
EXACTLY AS RECEIVED

LA THÈSE A ÉTÉ
MICROFILMÉE TELLE QUE
NOUS L'AVONS REÇUE

NL-339 (r. 82/08)

Canada

STRUCTURAL FABRIC AND URANIUM DISTRIBUTION IN SHEAR ZONES NEAR CARDIFF, ONTARIO

A Thesis

Presented to

the School of Graduate Studies

University of Ottawa

In Partial Fulfillment

of the Requirements for the

M.Sc Degree in Geology

By

M.K. Habib

1982

Professor A.J. Baer Thesis Supervisor

ABSTRACT

The pegmatite dykes cutting Grenville Supergroup along Highway No. 648(S) near Cardiff, Ontario, show narrow, concordant mylonite zones. Mylonites fall into two categories, called "A" and "B". A-type is high in uranium and contain magnetite and ilmenite stringers and ribbon-like quartz. B-type is uranium-poor and posses hematitic, plagioclase-rich bands alternating with deformed and recrystallized quartz bands. A-type mylonite normally shows SiO_2/Fe_2O_3 ratio (<20) distinct from B-type mylonite (>60).

Two generations of titanite, allanite and zircon are identified in the working area. First generation titanite, allanite and zircon show a concordant relationship with the mylonite fabric. Second generation titanite replaces magnetite and ilmenite along fractures. Second generation zircon and allanite grow over the old crystals and show a distinct chemical composition.

First generation titanite, allanite and zircon generally contain euhedral, microscopic radioactive inclusions. Second generation titanite does not contain radioactive inclusions, whereas second generation zircon and allanite show the presence of rounded microscopic inclusions on fission-track radiographs.

Uranium is accumulated in form of uraninite and uranothorite in A-type mylonite during and after the deformation. The interaction of magnetite and uranium-bearing solutions introduced in shear-zones during and after shearing causes the fixation of uranium. The reduction of uranium is accompanied by the oxidation of magnetite and the formation of hematite at the contact of radioactive minerals and magnetite.

CONTENTS

PLATES

FIGURES

TABLES

CHAPTER 1. INTRODUCTION

1.1 LOCATION

The thesis area lies about 18 kilometers south-west of Bancroft in Cardiff township. It consists of two separate areas "A" and "B". Area "A" stretches along Highway 648 (S), between Highway No. 121 and Highway No. 28. Area "B" lies roughly 5 kilometers north-east of area "A", (FIG. 1.0).

The region was mapped at a reconnaissance scale (1:126,720) by Adams and Barlow (1910). Cardiff and Faraday Townships were mapped by Hewitt (1957-1) at a larger scale (1:15,840).

1.2 PREVIOUS WORK

Ellsworth (1932) described various types of radioactive pegmatites and numerous uranium-thorium occurrences in the Haliburton-Hastings area. He also described various radioactive and rare-earth minerals and their genesis.

Lang (1952) summarized data on Canadian deposits of uranium and thorium. He briefly discussed the uranium mineralization of the Bancroft area.

A detailed description of the radioactive minerals in Bancroft area was given by Satterly (1955) with a classification of uranium deposits in the region. The description of various mining properties with their exploration history and production was given in detail.

Robinson and Hewitt (1958) summarized the geology of uranium deposits of the Bancroft region, with brief description on genesis, mineralogy and geochemistry of radioactive pegmatite dykes.

Fig. 1.0 Location Map (Geology after Hewitt, 1957-1)

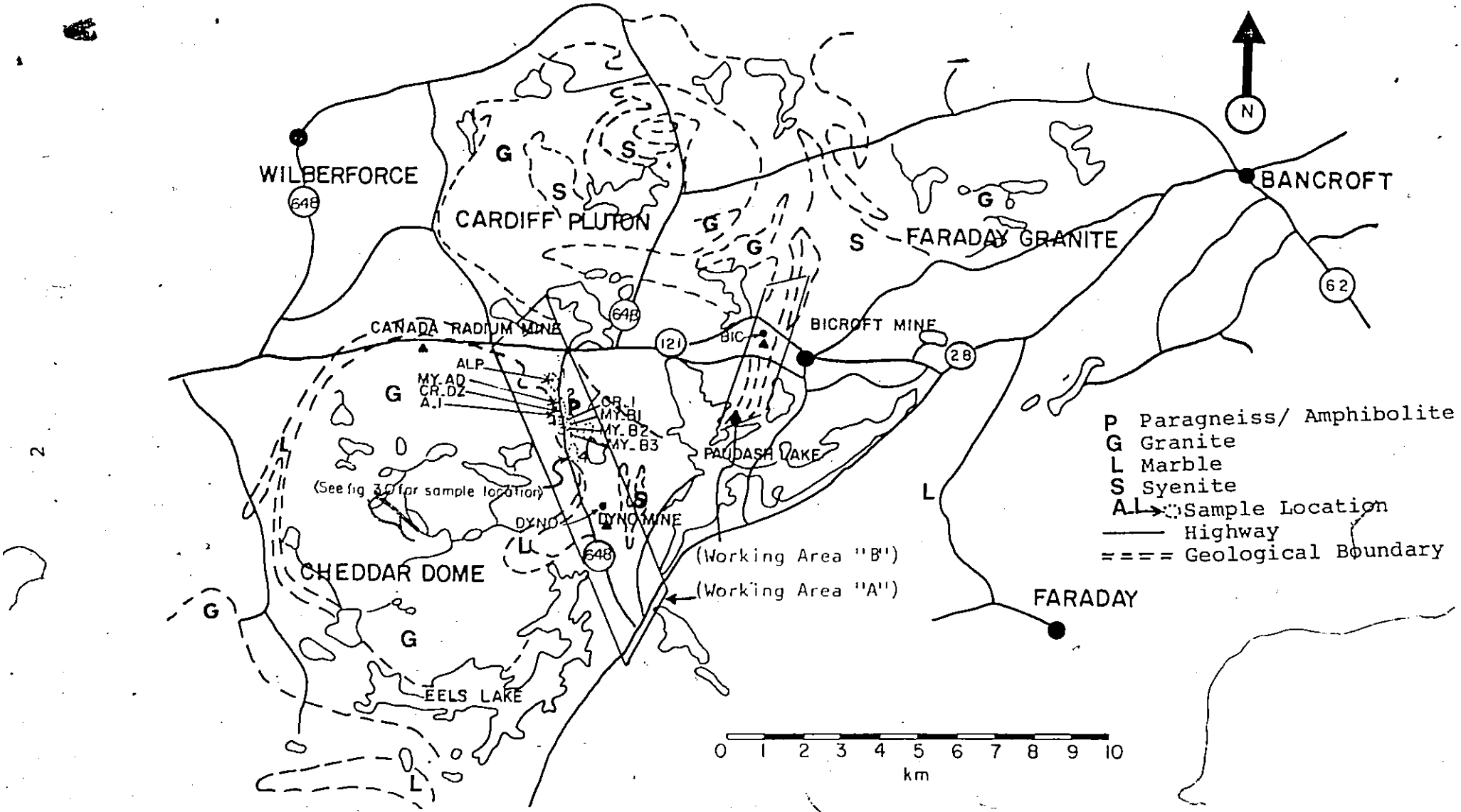

Later work by Lang et al. (1962), Little et al. (1972) and Hewitt (1967) described known radioactive occurrences in the Hastings-Haliburton area.

In the 1960's an extensive detailed mapping project was carried out by the Ontario Department of mines in the Bancroft region, and was published by Lumbers (1964, 1967).

Most of the work during the 1970's was done by Ruzicka (1971); Little et al. (1972); Bright (1974, 1975, 1976, 1977 and 1979); Robertson (1977); Gordon et. al. (1978); Gordon and Masson (1978).

Ruzicka (1971) compared Candaian and East-European uranium deposits and described various controlling factors for uranium localization in Haliburton-Hastings region.

Origin of the uraniferous pegmatite dykes in the area was discussed by Bright (1977) who suggested that the pegmatites were possibly derived from the melting of the basal arkosic material of the Grenville Supergroup, concentration and precipitation of uranium having taken place by the interaction of rising magma and wall rock.

Robertson (1977) discussed processes of uranium mineralization and related the uranium concentration processes to the mantled gneiss domes that he described as syn-Grenville orogenic granitic bodies.

Robertson (1977) described different types of uranium deposits, their mineralogy and genesis in the Bancroft area. He also discussed the past exploration history of the uranium-rich Bancroft area.

Gordon et al. (1978) studied uranium and thorium deposits and established a genetic relationship between the host rock (Grenville Supergroup metasediments) and the uranium mineralization. They

proposed like Bright((1977) that the basal arkose unit of the Grenville Supergroup was the source of the pegmatites.

After the present study was started, Bright (1979) proposed a regional stratigraphic control of uranium mineralization in Hastings-Haliburton Counties. In his opinion uranium deposits are stratigraphically concentrated in metavolcanis and the metasediments of the upper Hermon Group along the flanks of Cardiff and Faraday domes.

Masson and Gordon (1979) explained that structure and lithology control the mineralization, and that the deformation zones are generally restricted to particular stratigraphic horizons in the Bancroft area. They described the importance of shearing and deformation for uranium concentration, they further proposed the pegmatites as the immediate source and the Middle Precambrian granites or syenites as the primary source of uranium in the area. This however refutes Gordon's earlier idea (cf. Gordon and Masson, 1978) of the Grenville metasediments as the source of uranium.

Fowler and Doig (1979) dated (Rb/Sr whole rock) radioactive pegmatites from Dyno Mine and granite from adjacent Cheddar Pluton, and found a younger date for the pegmatite (970 Ma) than for the Cheddar Pluton (1200 Ma).

Although much work has been done on uranium deposits in the area and a relationship between shearing and uranium mineralization has been observed and described by some authors, detailed work, however, is lacking.

Two presentations have resulted from the present work (Fyson et al. 1979a and 1979b). They summarized various stages of the present investigation.

1.3 ACKNOWLEDGMENTS

The author wishes to acknowledge the help of Professor A.J. Baer, not only for his supervision and guidance throughout the entire investigation but also for his critical reading of the manuscript.

Grateful acknowledgment goes to Dr. D.D. Hogarth for his helpful suggestions at different steps during the research.

The writer is grateful to R.H. McCorkell of Bondar Clegg Company for providing literature and material and for his help in setting up the fission-track technique.

Thanks are also due to Dr. A.G. Plant of the geological Survey of Canada who has given his time in discussion and helped in qualitative microprobe analyses.

Thanks also go to Dr. J. Rimsaite of the Geological Survey of Canada for her helpful comments.

Grateful acknowledgment goes to Dr. W.K. Fyson for his critical reading of the manuscript.

The author also wishes to thank the following persons and organizations for their contribution to this thesis:

Ontario Geological Survey for providing the grant (Grant 47) for research;

Graduate student Nicholas Culshaw for his help during the field work;

Dr. Paul Mainwaring of Carleton University for microprobe analyses;

Mr. Ron Hartree for his help during the whole rock chemical analyses;

Mr. Edward Hearn for helping with photography and microphotography;

Mr. Naresh Kochhar for typing the thesis;

My wife Shahana for being the source of encouragement throughout the project.

1.4 PURPOSE

The purpose of this work was to reveal the relationship between the rock fabric and the uranium distribution, and to explain the behavior of uranium during shearing and deformation processes.

A close relation between shearing and uranium concentration has been described by several authors in Bancroft and other areas in Canada. However, a systematic study on a detailed scale to describe the controlling factors of uranium accumulation in shear zones was lacking.

The present investigation in the Cardiff area was aimed at delineating the phenomenon of uranium mobilization, accumulation and mineralization, along with deformation processes in pegmatites and other rocks.

1.5 FIELD WORK

The field study of regional structures and of the rock fabric associated with uranium distribution was undertaken during the field season of 1978.

Aerial photographs were used to select linear features or lineaments (possible magascopic structures) for field study. Such a line marked on the geological map of Ontario Department of Mines (Hewitt, 1957-1) as a fault line, was mapped at 1:1500 to delineate the distribution of pegmatites and uranium as a function of the distance from the lineament (Fig. 5.2).

The scintillation counter TV. 1A (McPhar Instruments Ltd.) was used for radioactivity measurements. The pegmatites were found to be uranium-rich and their U and Th values (on scintillation counter) were roughly uniform, therefore all radioactivity reported here are due to U + Th + background

(T2 threshold). Scintillation counter was placed in contact with the outcrops until the readings stabilized and a mean of three readings was reported at each point.

In the summer of 1979 the field study was narrowed down to the specific shear and mylonite zones in pegmatites and country rock. Field work included detailed mapping (scale 1:10 to 1:1).

Most of the measurements were made by making grids directly on the outcrops or on tracing paper lying over the outcrops. Narrow mylonite zones within pegmatite were marked along with the scintillation counts (Fig. 1.1). These measurements were taken at each point of the grid on tracing paper to show the distribution of uranium as a function of the distance from shear-zones (Figs. 1.1 and 1.1a) and variations along the shear zones.

In gneisses, amphobolites and marbles of the Grenville Supergroup scintillation counts were measured randomly as well as systematically along a line across the strike. Samples were taken by using a sledge hammer.

No mylonite zones were found in gneisses or amphibolites.

In undeformed pegmatites scintillation counts were measured in a line across the dyke and adjacent parts of the country rock. These measurements delineate the variation in uranium distrribution as a function of the distance from the margin of a pegmatite.

Samples were taken at several grid points across and along the mylonites in the pegmatite dykes (Plates 1.0 and 1.1) by using a portable hand drill (GSC type, J.K. Smith and Sons). Country rock was sampled with a sledge hammer.

FIG. 1.1 Mylonite zones in pegmatite show higher scintillation-counts (CPM) than adjacent, undeformed pegmatite. Radioactivity along line A-B is plotted in Fig. 1.1a. (Outcrop # 2, Fig.1.0)

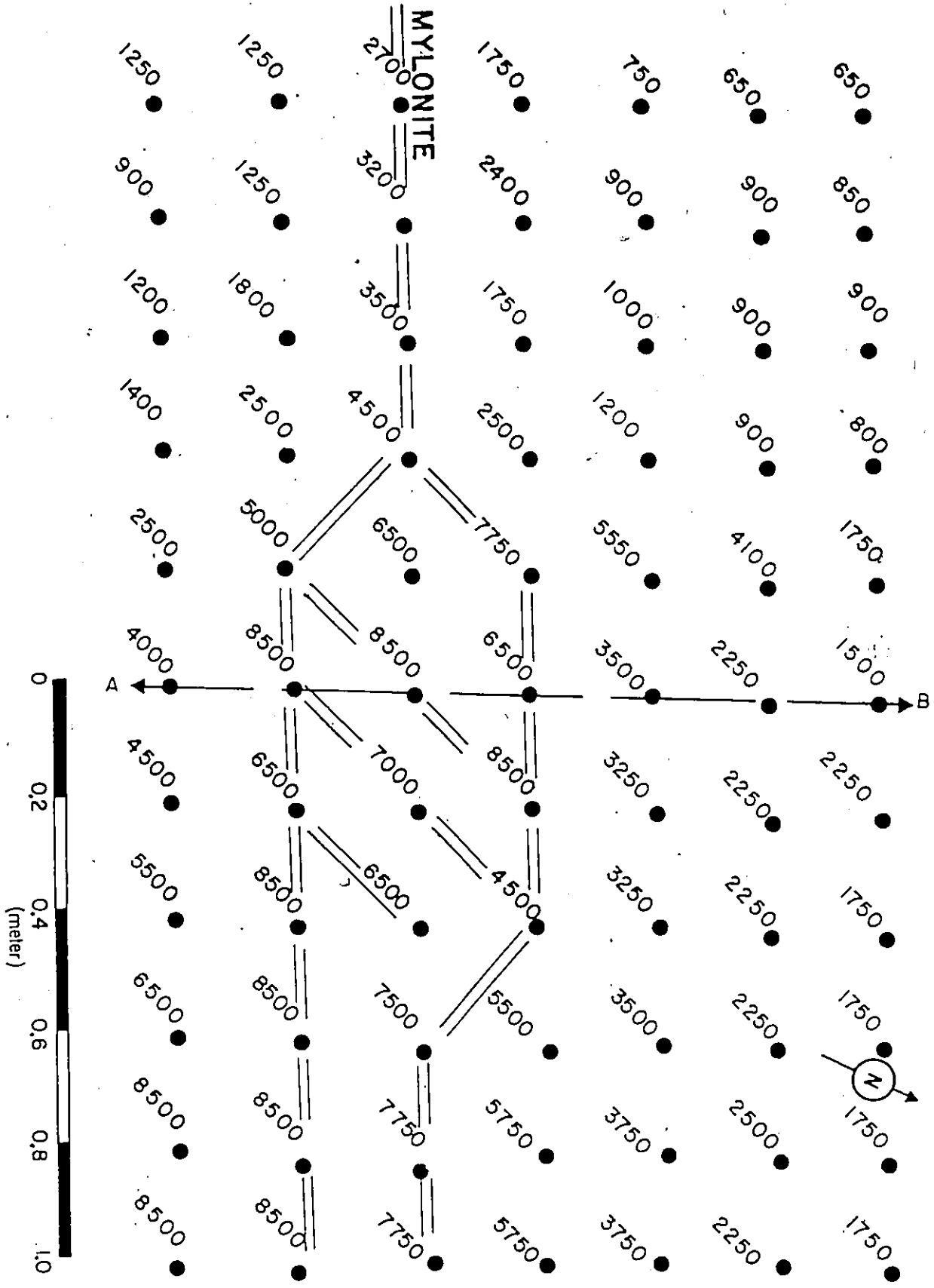

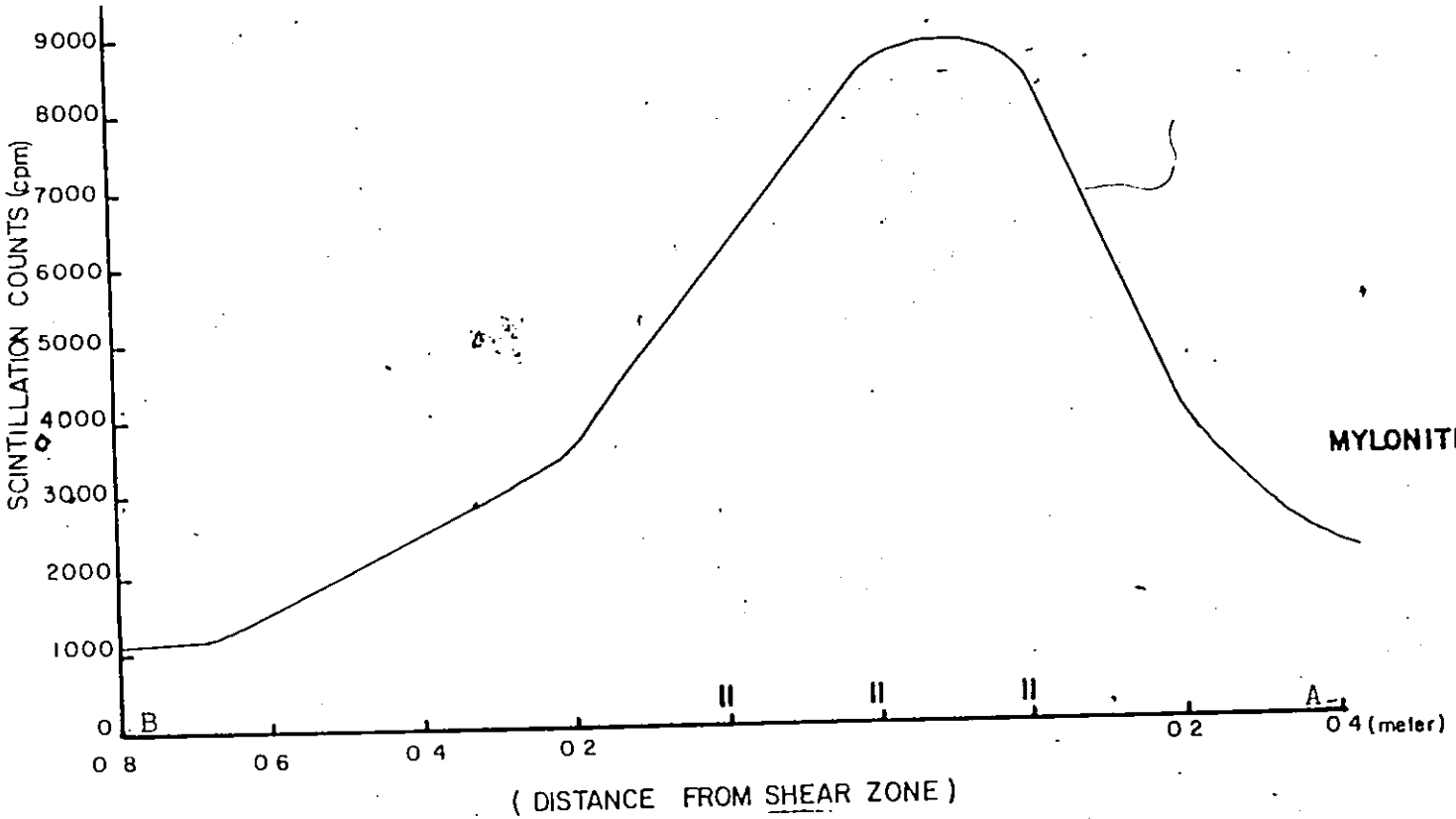

FIG. 1.1a Scintillation-counts versus distance from shear-zone.
(section along line A-B in fig. 1.1)

1.6 LABORATORY TECHNIQUES

Fission-track techniques were used to determine the concentration and the distribution of uranium in thin sections and slices of rock specimens. This method is based on the fission of U-235 in the specimen during bombardment with thermal neutrons in an atomic reactor (Fleischer et al. 1975). The fissioned fragments were recorded on a film (Lexan plastic) in contact with the specimen during the process. (Kleeman and Lovering, 1967). They leave a trail of damaged material or "fission-track" in the film (Plate 1.2). The tracks were enlarged by etching the Lexan overlays in 6N NaOH at room temperature for 20 to 30 hours (McCorkell, 1978, unpublished) and were observed with the microscope under high magnification (x100).

Gamma and alpha autoradiographs were prepared in addition to the fission-track radiographs to map the distribution of thorium and other radioelements (gamma ray and alpha particle emitters) along with uranium. Comparison of the autoradiographs and the fission-track radiographs of same specimens may help to reveal disequilibrium in the uranium decay series (McCorkell, personal communication, 1979).

1.6.1 AUTORADIOGRAPHS

Alpha and gamma autoradiographs were produced to map the total radioactivity of the specimens. Thin sections and slices of rock specimens were exposed to the radiation-sensitive film for a suitable length of time depending on the radioactivity of the rock determined in the field by using scintillation counter (TV.1A) (Table 1.0).

GAMMA AUTORADIOGRAPHS: They were obtained by exposing the cut slabs (maximum 10 cm x 8 cm) and thin sections of the rocks to the X-ray film (Kodak Industrial) in a dark room. Thin sections were generally exposed for a time duration ranging from one week to two weeks, whereas the slices were exposed for 24 to 48 hours. An image of the gamma ray emitting phases was obtained after the normal processing of X-ray film.

ALPHA AUTORADIOGRAPHS: They were produced in a similar way by exposing rock slices (maximum 8 cm x 6 cm) and thin sections to the cellulose nitrate film (Kodak LR-115 type 11) for two to three days to two to three weeks respectively. After exposure, films were etched in 2.5 N NaOH at 60°C for 115 minutes (McCorkell, 1978, unpublished) to enlarge the pits produced by alpha particle radiation.

In each case, the specimens and film were matched accurately to locate radioactive sites.

1.6.2. FISSION-TRACK RADIOGRAPHS

The fission-track radiographs were produced mainly by following the unpublished text and the personal instructions of Dr. McCorkell of the Bondar Clegg Company Limited.

Thin sections and slices of the rock specimens were prepared in form of discs of about 20 mm in diameter. A sheet of Lexan plastic of similar diameter was placed on top of each thin section.

Table 1.0 Length of exposure and neutron dose for different specimens.

Radioactivity (cpm)	Rock Description	Length of Exposure					
		Slices			Thin sections		
		Gamma**	Alpha**	FTR*	Gamma**	Alpha**	FTR*
<200	No radioactive or accessory mineral present in hand-specimen or in thin section.	48 hrs.	60 hrs.	90 min.	14 days	20 days	120 min.
200-500	A few accessory minerals present	30-45 hrs.	40-55 hrs.	60 min.	10-14 days	18-20 days	90 min.
500-1000	Accessory minerals abundant	30 hours.	50 hrs.	-	10 days	18 days	60 min.
1000-5000	Accessory minerals abundant with radio-active inclusions	24-30 hrs.	40-50 hrs.	-	7-10 days	14-18 days	45 min.
>5000	Coarse grained radioactive minerals present.	24 hrs	48 hrs	-	7 days	14 days	15-30 min.

* Fission-track Radiograph.

** Autoradiographs.

Rock slices were covered with Lexan plastic on both sides.

Each specimen with its Lexan overlay was wrapped in aluminium foil to prevent contamination by uranium from adjacent specimens. The uranium concentration within aluminium foil itself was found to be very uniform, therefore it does not affect the measurements (McCorkell, 1978, unpublished).

Specimens were filled in irradiation capsules along with two uranium standard glasses (prepared by the National Bureau of Standards, USA) mounted in epoxy and placed at each end of the capsule. They were irradiated in the Slowpoke Reactor of the Atomic Energy of Canada Limited in Ottawa.

A thermal neutron flux of 2.8×10^{11} n cm^{-2} s^{-1} was used to irradiate the capsules for different lengths of time (Table 1.0). Lexan overlays were removed from irradiated specimens and etched in 6 N NaoH at room temperature for 20 to 30 hours to enlarge the fission-tracks (McCorkell, 1978, unpublished).

Detailed prints of the location of uranium-bearing minerals and therefore of microstructures were obtained. Each uranium-containing mineral present in the rock could be located by its shape on fission-track radiographs (Plates 1.3, 1.3R, 1.4 and 1.5).

General distribution of tracks was studied under reflected light by looking at specimens covered with accurately oriented Lexan overlays. Detailed studies were made on thin sections in a similar way, by using transmitted light under high magnification.

The uranium concentration of each specimen was calculated by comparing the number of tracks over a unit area in the Lexan overlay of a specimen (fission-track radiograph) with the number of tracks in overlays

of standard glass, irradiated together with the specimens. The density of tracks in the Lexan overlay is proportional to the uranium concentration of the specimen.

The variation in the neutron flux along the length of the capsule can be measured by comparing the track density over uranium standard glasses at both ends of the capsule.

1.6.3 URANIUM STANDARD GLASSES

For the measurement of the uranium concentration, NBS standard glasses (prepared by National Bureau of Standards, US Department of Commerce) were used as reference material.

These glasses are prepared to be used as analytical standards for 61 elements. Four sets of NBS glasses are available, SRM (Standard Reference Materials) 610 and 611, 500 ppm in the oxide of each element, SRM 612 and 613, 50 ppm in each element and SRM 614 and 615, 1 ppm in each, and SRM 616 and 617, 0.02 ppm in the oxide of each element. The actual values of these elements differ from these values to a certain extent. The uranium used in these glasses is depleted in U-235 (N.B.S., 1970). The corrected values of uranium concentration for fission-track determinations, provided by National Bureau of Standards (U.S. Department of Commerce) are reported here.

U^{235}/U^{238}	(normal)	- 0.7256
	(N.B.S. glass 612)	- 0.2392
	(N.B.S. glass 614)	- 0.2792
	(N.B.S. glass 610)	- 0.2376

No.	Element concentration	Corrected values for F.T. U determinations
SRM 610	500 ppm	151.11 ppm
SRM 612	50 ppm	6.37 ppm
SRM 614	50 ppm	0.33 ppm

1.6.4 FISSION-TRACK DETERMINATION OF U IN WHOLE ROCK

Existing data on the uranium contents of different rocks show considerable variations. Some of these discrepancies were discussed by Fisher (1970).

This author made several attempts to compare the fission-track method with microprobe techniques for determination of uranium content of individual minerals (Chapter 4) and found several discrepancies. Thin sections and rock slices were used to determine the uranium content of individual crystals. Because of the heterogeneous distribution of uranium in the rocks, it is difficult to analyse the data in terms of average uranium concentration of a rock.

Fisher (1970) described the technique of homogenized fission-track determination of uranium in whole rock samples. He prepared disks by compressing rock powders (2000 lb/in^2). After irradiation the intensity of induced tracks was measured in the covering plastics. He discussed the problems of tracks clustering due to inhomogeneous distribution of uranium that make it difficult to measure the average uranium concentration. The present author was able to avoid fission-track clusters by melting powdered rocks and preparing homogenized glass disks. The present technique was also compared with the method applied by Fisher (1970) (Table 1.1).

To prepare fused glasses the rocks were crushed and then finely ground in the shatter box, each specimen for three minutes. 1.5 gram of rock powder was weighed in a platinum crucible with 0.5 gram of $LiCO_3$ and 4.5 grams of LiB_4O_7 (flux). Platinum crucibles containing the mixture of the rock powder and fluxes were then heated for 9 minutes on a Bunsen burner The melt was stirred automatically for 9 minutes and then molded into disks.

Fused glass disks, each covered with Lexan plastic sheets on both sides were completely wrapped in aluminium foils. They were packed in capsules for irradiation along with two uranium standard glasses (prepared by National Bureau of Standards, U.S.) mounted in epoxy, placed at each end of the capsule.

Induced track densities were counted in each Lexan overlay after irradiation and etching (Chapter 1, art. 1.5). No clusters were found in any specimen. Tracks were uniformly distributed throughout the disk. Note that the concavity produced during the cooling of molds, causes an improper contact between the Lexan film and the specimen surface, but the opposite even surface of the same disk does not show such variations.

1.6.5 COMPARISON OF AUTORADIOGRAPHS AND FISSION-TRACK RADIOGRAPHS

Although gamma radiography is a faster technique, it has several disadvantages. The matching of radioactive image with the specimen is difficult, because gamma rays form an image on the film even when the uraniferous material is lying several millimeters beneath the surface of the sliced specimens (McCorkell, 1978, unpublished).

Table 1.1 Examples of fission-track U determinations in homogenized rock specimens from Highway No. 648(S) near Cardiff, Ontario.

Sample No.	Rock Description	U ppm FGD*	U ppm RPP*
MY-A5	Mylonitized pegmatite (A-type)	217.9	n.d
A-1	Mylonitized pegmatite (A-type)	514.0	300-750 Av. 565
PW.MG1	Mylonitized pegmatite (A-type)	755.0	n.d
MY-B1	Mylonitized pegmatite (B-type)	43.7	n.d
ALP	Allanite-rich underformed pegmatite	500.0	700-950 Av. 825
PE-78	Undeformed pegmatite	44.0	n.d
C-1	Undeformed pegmatite	63.0	n.d
Peg-2	Undeformed pegmatite	10.5	n.d
PE-16	Amphibolite (country-rock)	3.1	n.d
CR-PW2	Amphibolite (country-rock)	0.8	n.d
CR-DZ	Quartz-biotite gneiss	0.5	n.d

n.d : not determined

* FGD: Fused glass disks

* RPP: Rock powder pellets

It also needs a darkroom since the film is light-sensitive.

Alpha autoradiographs require a longer time of exposure but the technique is more specific for the uranium-thorium decay series.

The fission-track method has several advantages over autoradiographs. Firstly it gives the distribution as well as concentration of uranium. Secondly it is sensitive enough to measure uranium content as low as 10 ppb (McCorkell, 1978, unpublished). A comparison of both techniques is given in Table 1.2.

1.6.6 IDENTIFICATION OF RADIOACTIVE AND U-BEARING ACCESSORY MINERALS

Most of the coarse-grained accessory minerals were identified under the microscope on the basis of their optical properties. Fine-grained zircon, titanite, allanite, monazite and uranothorite were identified by using the X-ray powder camera technique. For this purpose, mineral grains in thin sections were powdered by scratching them with a sharp needle, under the binocular microscope. The powder was picked up from the thin section by means of a fine glass spindle, dipped in vaseline. It was then analyzed in the 57.3 mm diameter Philips X-ray diffraction camera with Ni filtered copper radiation at 40 Kv and 20 m.A for three hours.

Coarse-grained metamict (isotropic) minerals were separated under the binocular microscope and were heated at 1000^{o}C for one hour in a small charcoal-lined crucible fitted in another crucible to create a reducing environment (Adams and Sharp, 1970). After heating, mineral grains were powdered and analyzed in the X-ray diffraction powder camera.

Table 1.2 Comparison of Alpha and Gamma Autoradiographs and Fission-Track Radiographs.

Properties	Gamma ARG*	Alpha ARG	Fission-track Radiograph
Recording Film	X-ray Industrial	Cellulose nitrate, LR-1	Lexan plastic
Exposure length			
1. slabs	24 to 48 hrs	48 to 60 hrs	10 to 90 min
2. thin sections	7 to 14 days	14 to 20 days	10 to 120 min
Needs dark room?	Yes	No	No
Processing			
1. chemicals	Normal processing	Etching with 2.5 M NaOH	Etching with 6 N NaOH
2. time length	20 min.	120 min	5 to 25 hrs
3. temperature	Room temp	60° C	Room temp
Quantitative?	No	Yes	Yes
Discriminates U from Th?	No	Possible	Yes

* Autoradiograph.

Microprobe analyses were performed on most common accessory and radioactive minerals like titanite, zircon, allanite and uranothorite (Table 4.2, 4.7, 4.9 and 4.16. See also page 60). They were analyzed by Dr. Paul Mainwaring of Carleton University on microprobe (Cambridge Mark 5) by using EMPATR V11 program. Atime interval of 120 seconds was used at 20 kV. Width of the beam used was 1 to 2 nanometers. The characteristic lines used for different elements are as follows :

U and Th	:	Mα
Zr	:	Lα
Ti	:	Kα
Si, Na, Ca, Fe	:	Kα
Ce, La, Nd, Sm	:	Lα

CHAPTER 2. GEOLOGY

2.1 GENERAL GEOLOGY

The Bancroft area is located near the southwestern margin of the Grenville province in the Canadian Shield. It is characterized by high-grade, regionally metamorphosed rocks of Precambrian age (Baer et al.1970).

The oldest rocks exposed in the area are possibly the Late Precambrian supracrustal rocks of the Grenville Supergroup. They are probably unconformably overlying a Middle Precambrian basement gneiss complex, not exposed in the working area.

The supracrustal rocks are intruded and replaced by various rocks ranging in composition from gabbro to granite.

The area was subjected to the Grenville orogeny (950 Ma K/Ar) and the rocks were metamorphosed under conditions ranging from lower amphibolite to upper amphibolite facies.

Grenville Supergroup: These are Late Precambrian supracrustal, possibly metasedimentary rocks with minor metavolcanic layers. Most of the metasediments are quartzo-feldspathic gneisses and amphibolites with minor quartzites and marbles. Metavolcanics generally occur as thin interbedded and intercalated zones of pyroclastics and mafic to intermediate flows within metasediments (Gordon et al. 1978).

The stratigraphic sequence and the lithology of the units are variable but a generalized lithostratigraphic succession of the Grenville Supergroup established by Bright (1977) may enable one to make a correlation of major units in the area.

The Anstruther Lake Group may be the oldest division of the

Grenville Supergroup. It is further divided into lower and upper sub-units (Bright, 1976). The lower sub-unit mainly composed of magnetite-rich and biotite-poor quartzo-feldspathic gneiss, is exposed in the Eels Lake area (Bright, 1977). The unit was correlated with the Faraday Granite (Gordon et al. 1978).

The Anstruther Lake Group is stratigraphically overlain by the Hermon Group (Lumbers, 1967) and by the Mayo Group (Hewitt, 1957), the youngest subdivision of the Grenville Supergroup.

Four batholithic complexes are mantled by the supracrustal rocks of the Grenville Supergroup (Fig. 5.1). These bodies are called the Anstruther Batholith, the Cheddar Dome, the Cardiff Plutonic Complex and the Faraday Granite. Among these four bodies, only the Cheddar and, north of it, the Cardiff belong in the area discussed here.

Cheddar Dome: Hewitt (1957) described it as a circular "double domed" intrusive pluton, having migmatized zones formed by the lit-par-lit injection of magmatic material into metasediments. Bright (1977) explained its origin by partial melting of basal arkosic material of the Grenville Supergroup. Recent work by Culshaw (personal communication, 1980) suggests that Cheddar is a roughly cylindrical obliquely plunging diapir which has been deformed after its emplacement.

The Cheddar Dome is situated to the north of Anstruther Batholith, on the boundary of Monmouth and Cardiff Townships. It consists of quartz monzonitic to granitic rocks and their gneissic equivalents. It is mantled by steeply dipping paragneisses, marble and amphibolites intruded by granitic to syenitic rocks.

Cardiff Plutonic Complex: It is a 10 km wide, oval-shaped centre of unexposed basement uplift and granitic intrusions (Bright, 1979). It consists of three plutonic bodies, the Centre Lake and Monk Lake Granites and the Deer Lake Syenites.

The granites are massive to foliated leucocratic quartz monzonitic to granitic sills. The Deer Lake Syenite lies to the south of Deer Lake and consists of alkaline syenites. The Cardiff Pluton is also mantled by the Grenville Supergroup rocks. Wide bands of these rocks that occur within the plutonic complex were described by Hewitt (1957) as infolded metasediments and metavolcanics. The recent work of Culshaw (personal communication, 1980) suggests that the Cardiff is an incomplete cylinder-shaped plunging body of granodiorite.

Bright (1979) described a thick sequence of coarsely crystalline pegmatitic arenaceous metasediments as the lowermost unit of the Grenville Supergroup overlying an inferred basement gneiss complex in the core of the Cardiff Dome. He correlated this sequence with the Anstruther Lake group. This unit is overlain by a thick sequence of clastic, siliceous to calcareous, coarsely recrystallized metasediments with mafic to alkaline volcanic rocks. It was correlated with the Hermon Group by Bright (1979).

2.2 RADIOACTIVE PEGMATITES AND U DEPOSITS

The working area lies in a belt of Grenville Supergroup metasediments between the Cheddar Dome to the west and the Centre Lake Granites of Cardiff Pluton to the east and northeast (Fig. 1.0).

All uranium occurrences in the area lie in the pegmatite dykes cutting paragneiss and amphibolites. They are exposed along Highway No. 648(S) in Cardiff Township in low lying outcrops striking N30^{o}W to N20^{o}E and dipping subvertically (Plate 2.0).

Pegmatite dykes range from a few inches to several tens of feet in width, roughly uniform along the strike of dyke (Plates 1.0, 1.1 and 2.1). Pegmatites are variably deformed. They are often branched and they cut gneisses at moderate to high angles and along sharp contacts (Plates 1.0, 1.1). They generally contain xenoliths of the country rock (Figs. 2.1 and 2.2).

Most of the uranium occurs in form of inclusions within widely distributed and locally concentrated accessory minerals, titanite, "leucoxene", allanite, zircon, cyrtolite and monazite. Uraninite and uranothorite are often associated with magnetite and ilmenite within mylonite zones in pegmatite.

The most important uranium occurrence in the area, the Canadian Dyno Mine, was active from 1954 to 1960. It produced 802,998 pounds of U_3O_8 (Hewitt, 1967) from the pegmatite dykes. The mine is located near Highway No. 648(S) 4.5 km south of Highway No. 121 and 3.5 km north of Highway No. 28 (Fig. 1.0).

Radioactive pegmatites cutting gneiss and amphibolite are deformed and very similar to those exposed along Highway No. 648 (S) described earlier.

Another important uranium occurrence is the Canada Radium Mine (Fig. 1.0) incorporated in 1932, that was in operation during different periods until 1955 (Hewitt, 1967).

The Radium Mine property lies on the northeast edge of the Cheddar Dome in paragneiss and amphibolites. Pegmatite dykes are similar to those of Canadian Dyno Mine pegmatites, but they often contain local hornblende and pyroxene-rich zones.

There are a number of other uranium showings in the area. They all occur in similarly sheared, magnetite-ilmenite and quartz-rich pegmatites

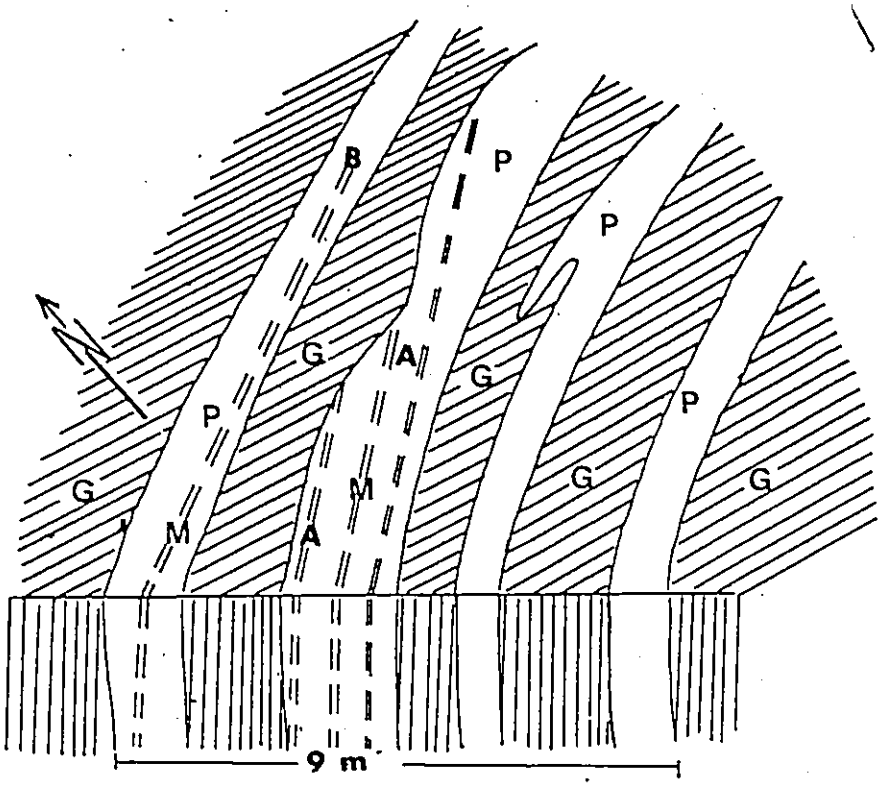

FIG. 2.1 Northeastern part of outcrop (No. 3, in fig. 1.0) along Highway No. 648 (S). (G: gneiss, P: pegmatite, M: mylonite). (A: A-type mylonite and B: B- type mylonite)

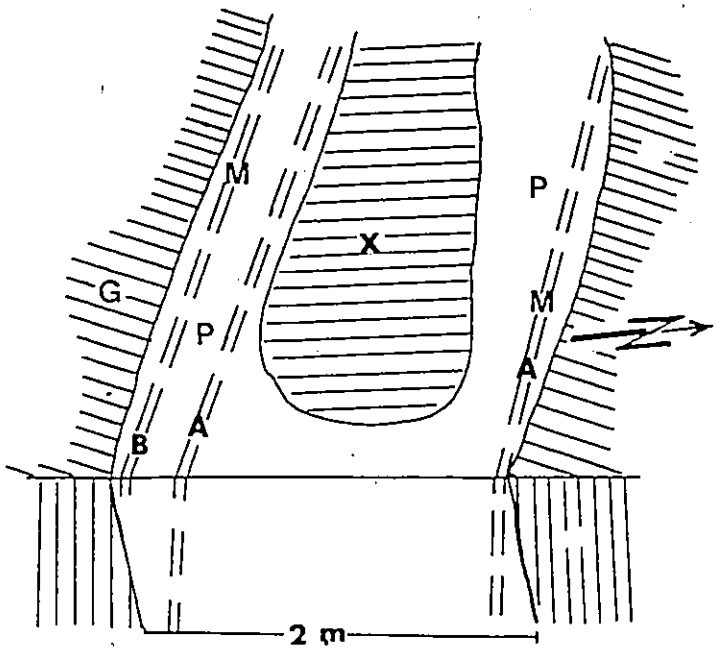

FIG. 2.2 Southwestern part of the above outcrop. A pegmatite dyke (P) showing mylonite zones (M) and a large xenolith(X) of the country rock (G).(A:A-type mylonite; B:B-type mylonite).

very similar to those of Canadian Dyno Mine and Canada Radium Mine. These pegmatites are exposed at a number of places in open pits, shafts and trenches in the working area.

CHAPTER 3. PETROGRAPHY OF PEGMATITES

Pegmatite dykes cut across the paragneiss and amphibolites of the Grenville Supergroup. They range from a few centimeters to several tens of meters in width and the exposed thickness varies from half a meter to a maximum of 10 meters in the working area (Fig. 3.0).

They are normally coarse grained, leucogranitic, variably deformed pegmatites, ranging from slightly deformed to highly recrystallized mylonites. They may show changes of mineralogy and grain size within a fraction of a centimeter. They are classified into two groups accordingly: 1) the microcline-perthite bearing, partly deformed pegmatites, and 2) the mylonitic pegmatites.

1) Microcline-perthite bearing pegmatites: Microcline forms more than 60% of the rock and occurs as large crystals up to several centimeters in diameter. A graphic intergrowth of quartz and microcline is generally observed. In thin sections microcline very often shows plagioclase exsolution.

Quartz makes up to 30% of the rock. It occurs in various grain sizes, shows strain effects and recrystallization, whereas the central parts of grains are strained and show undulatory extinction. In moderately deformed rocks quartz may occur as lens-shaped, elongated grains which show recrystallization at their margins only.

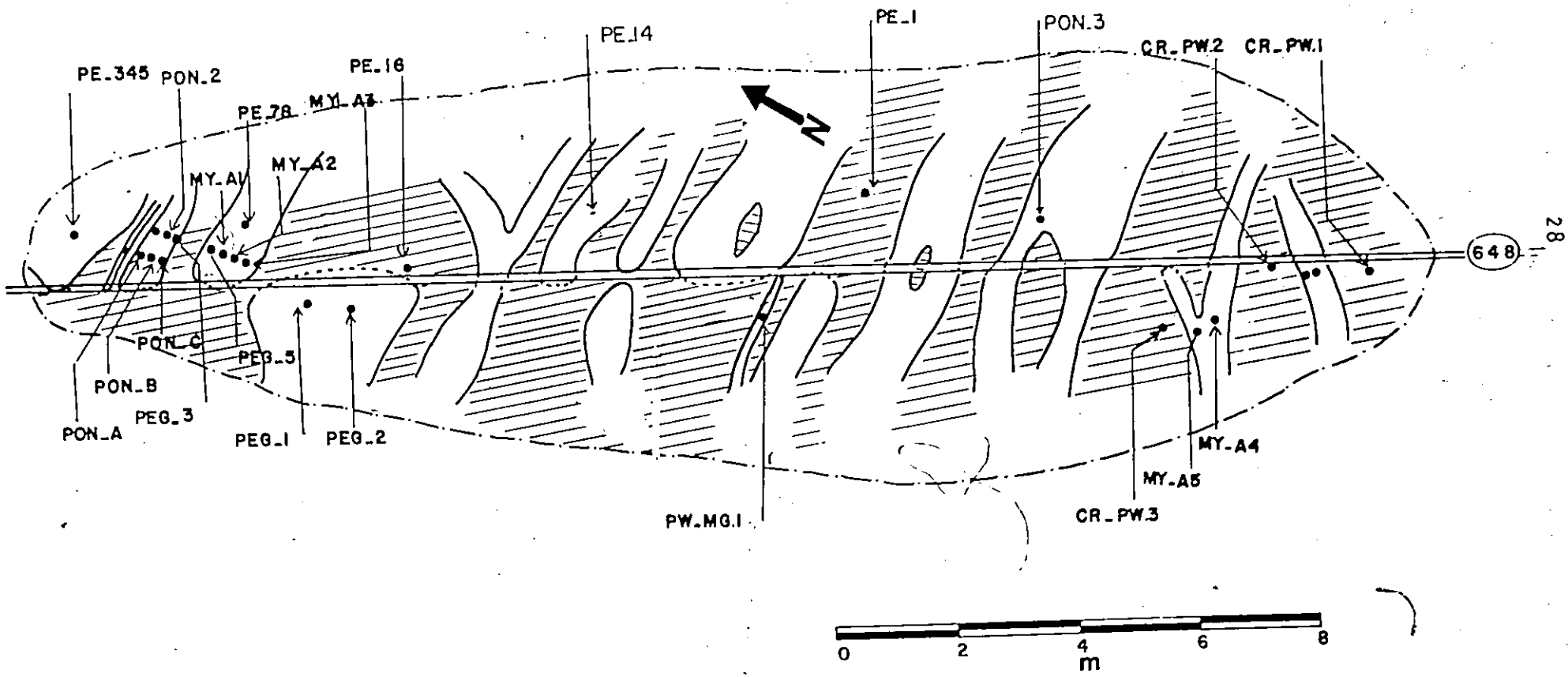

Fig. 3.0 Detailed sketch of outcrop (No. 4 in Fig. 1.0) along Highway No. 648(S) showing the sample locations. (pegmatites: white, host-rocks: lined)

Plagioclase forms 10-15% of the rock, occurs as small (0.5 mm to 2.5 mm in diameter) anhedral grains generally kinked and bent, with fine grained, possibly recrystallized, plagioclase at their margins. They generally occur in between large microcline crystals.

Most of the plagioclase is oligoclase (An 10-20) (Michel-Lévy method). Plagioclase contains hematite in cleavage and twin planes which give a red appearance to the plagioclase-rich zones. The mafic constituents include biotite, hornblende, pyroxene and epidote. They do not exceed 3% on average but they may locally represent as much as 15% of the rock.

Important accessory minerals are titanite, allanite and zircon with less abundant monazite, cyrtolite and pyrite. A general association of titanite and leucoxene with magnetite and ilmenite has been observed almost everywhere in pegmatites and in country rock.

The amount of accessory minerals is quite variable, and ranges in general from 5 to 25%. An increased abundance of accessory constituents with increasing deformation is generally observed. More than one generation of titanite, allanite and zircon is evidenced by their concordance and discordance with mylonite fabric in pegmatite. Their genesis and uranium distribution is described in this chapter and in Chapter 4.

2) Mylonitized pegmatites: Mylonites are in widely distributed, long, narrow (0.5 cm to 10 cm in width) zones in the pegmatites. They are roughly parallel to the margins of the dykes (Plates 1.0, 1.1).

Two types of mylonites are distinguished in the working area "A". One is highly radioactive, characterized by the presence of abundant magnetite

Stringers and smoky quartz. It is called "A" type (Plate 3.1) and the other Less radioactive type (radioactivity measured in field) with hematitic, kinked plagioclase-rich bands is the "B" type (Plate 3.2).

The presence of magnetite, ilmenite or hematite in A and B type mylonite explains the different state of oxidation of iron in the two types.

A and B type mylonite may occure within a single pegmatite dyke side by side (Fig. 2.1 and 2.2) but one does not grades into the other longitudinally.

2a) "A" type mylonites : They contain light bands of varying shades and width (0.05 to o.5 cm. wide) with dark stringers (0.1 to 0.8 cm.wide) and boudins within or alternating with light bands. A large number of uraniferous minerals occur within these bands. At least two different generations of titanite, allanite and zircon are identified in these mylonites. First generation minerals are concordant to the mylonite fabric (Plates 3.3 and 4.1). Second generation titanite generally replaces magnetite and ilmenite in fractures. Second generation zircon and allanite grow over the old crystals (Plates 3.10 and 3.11) and show uranium enrichment and a distinct chemical composition(Table 4.7 and 4.9).

Light bands: Light bands in these mylonites consist of highly deformed and finally recrystallized quartz and more rarely of large lens-shaped strained quartz with recrystallized margins (Plate 3.1). These bands make upto 75% of the A-type mylonite.

Dark bands: Dark bands make 5% to 15% of the A-type mylonites. They consist of elongated and deformed magnetite and ilmenite . Under reflected light with crossed nicols , magnetite appears to be isotropic and can be distinguished from anisotropic ilmenite. The latter shows twinning and recrystallization and lamellae of exsolved hematite (Plate 3.4).

Magnetite shows some replacement by hematite along the cracks and at the contacts with uranium-bearing minerals (Plate 3.5). It is generally characterized in thin sections by a large number of cracks and pits. These bands occasionally contain fine-grained biotite and hornblende along their margins.

In some cases radioactive mylonites consist almost entirely of recrystallized smoky quartz with little or no feldspar and 5% magnetite.

Accessory minerals in "A" type mylonites: Nearly 60% of the total uranium in the pegmatites resides in accessory minerals in form of tiny radioactive inclusions. Accessory minerals like titanite (better than sphene) (Fleischer, 1980) and allanite occur within magnetite-ilmenite bands or at the contact of light and dark bands (Plate 3.1, 3.3). Zircon, cyrtolite, monazite and apatite mainly occur within recrystallized quartz zones (Plates 3.6, 3.11a and 7.0).

Titanite: two generations of titanite are identified in the mylonites. Old titanites are large, fractured and generally contain a number of inclusions whereas younger titanites are smaller, clear and generally occur at margins or in cracks within magnetite-ilmenite grains. (Plate 3.9).

First generation titanite crystals are euhedral to subhedral, mostly fractured and partly altered. They range from 0.1 cm to 0.5 cm in diameter. 80% of the titanite crystals occur within magnetite and ilmenite bands, where they are roughly oriented along the mylonitic fabric. They show lamellar twinning and pressure-induced parting. In some cases the parting planes are bent (Plate 3.7).

In some cases, twin and parting planes and fractures are occupied by magnetite and recrystallized quartz (Plate 3.7). The former alters to cloudy semi-opaque material (leucoxene). Few titanite crystals show alteration to leucoxene along fractures (Plate 4.2).

The titanite crystals generally contain small euhedral inclusions of uranothorite, monazite and rarely uraninite (Plate 1.5).

Younger titanite crystals are small (0.01 cm to 0.25 cm) and mostly occur at margins or in cracks within magnetite and ilmenite (Plate 3.9). They do not show partings and are free of inclusions. These titanites were possibly formed after, or late in the deformation process.

Allanite: Allanite is present as large (0.3 cm to 6 cm) euhedral to subhedral crystals, characterized in thin section by their cigar-shaped appearance, a network of fractures, and a large number of inclusions such as uranothorite, cyrtolite, monazite and rarely uraninite. A number of radiating fractures originate from these inclusions and shatter the allanite crystal.

Alteration and metamictization are commonly observed in allanite. They are caused by the breakdown of crystal structure by the radio-active bombardment from contained inclusions.

80% of the allanites show a narrow zone at their margins, characterized by lighter colour (Plate 3.10), lower birefringence and higher uranium content (Chapter 4) than the inner, dark, rusty-brown zones.

The narrow outer zone has a chemical composition different from the core (Table 4.7). However, concentrations of uranium and rare-earths are variable along this zone (Tables 4.6 and 4.7). Optical and

chemical differences between the rims and cores in the allanite crystals reflect more than one stage of crystal growth. The uranium and rich margin is possibly an overgrowth on an older rusty-brown core, formed before the deformation process.

Zircon: Zircon occurs as subhedral to euhedral crystals ranging from 0.05 to 0.10 cm in diameter. It is almost always found within deformed and recrystallized quartz-rich zones in mylonites. Zircon crystals are mostly enveloped by a thin band of hematite or limonite (Plates 3.11 and 3.11a).

Nearly 80% of the zircon crystals show clear cross-cutting relationships and about 20% crystals appear to be concordant with the mylonitic fabric.

Three different varieties of zircon have been identified on the basis of their optical properties, chemical composition and uranium content.

1) Body-Zoned Zircons: These are generally coarse grained, non-metamict zircons, possibly of post tectonic origin as evidenced by their discordance with the mylonite-fabric. They show some dark bands (non-metamict). Uranium is evenly distributed across the crystals (Chapter 4). The distinct zone is probably due to variations during crystal growth.

2) Rim-Zoned Zircons: These zircons have zoned, often incompletely developed rims (Plates 3.11 and 3.11a), and unzoned, generally cloudy and fractured cores. Zoned rims are similar to the body-zoned zircons described earlier. Some crystals do not show clearly zoned rims.

On fission-track radiographs 60% of the rim-zoned zircons show clear evidence of uranium enrichment in zoned rims. Uranium-rich rims are optically and chemically different from the cores (Table 4.9). These zircons reflect more than one stage of crystal growth.

Uranium-rich overgrowths in zircons studied and described by different authors are briefly discussed in Chapter 4.

Microprobe and fission-track analyses and studies under the microscope suggest the formation of new zoned zircons as separate crystals or overgrowths on earlier formed unzoned zircons. They have a complicated, partly discordant (Plate 3.11) relationship with the mylonite fabric. This suggests an origin, early in the deformation process. None of the zircon cores show evidence of detrital origin. The cores are most probably pre-tectonic igneous zircons.

3. Metamict Zircons (cyrtolite): These are euhedral to rounded (non-detrital) crystals. They generally show a large number of microscopic inclusions which appear as tiny clusters on fission-track radiographs. They are mostly unzoned. Cyrtolite may occur as inclusions within larger accessory minerals like titanite and allanite (Plates 3.8 and 4.1).

Monazite: Monazite is less abundant than other accessory minerals. It normally occurs as small grains (0.01 cm to 0.05 cm) and occasionally as larger euhedral crystals (0.01 cm to 0.25 cm) within recrystallized quartz-rich zones in mylonites. Most of the monazite bears a cross-cutting relationship to the mylonitic fabric, but the larger crystals very often show a concordance with the fabric.

Apatite: Apatite is a less important uranium-bearing mineral of most probably pre-tectonic origin because of its concordance with the fabric of mylonite. It occurs as small colourless euhedral to subhedral crystals in mylonitized pegmatites.

Rutile: Rutile is a rare mineral, occurs as thin bands over the

margins of ilmenite and magnetite and appears to have formed late during the deformation process.

2b) "B" type mylonites: Unlike "A" type, "B" type mylonites do not contain magnetite and ilmenite stringers. Under reflected light they show hematite-rich irregular bands which alternate with light-coloured zones showing shades of hematitic stains. A few magnetite grains may occur in these mylonites.

Red (hematite-rich) bands: Under transmitted light these bands appear to be composed of kinked and bent plagioclase crystals. Hematite occurs in cleavage and twin planes and at grain boundaries. A few larger crystals of potash feldspar (0.25 cm to 0.5 cm) occur in this zone.

Light bands: Light bands contain elongated, deformed and recrystallized quartz. The quartz bands are generally discontinuous and shorter than in "A" type mylonite, and contain some hematitic coating in fractures and along boundaries of larger grains. Quartz forms up to 30% of this zone.

Microcline ranges from 0.3 cm to 1.25 cm in diameter. It generally shows perthitic texture and makes up to 60% of light bands.

Accessory minerals: Accessory minerals are less common in "B" type mylonites and do not exceed 5% of the rock. Apatite is a common mineral whereas titanite and zircon are comparatively less common.

CHAPTER 4. URANIUM DISTRIBUTION IN INDIVIDUAL MINERALS

4.1 URANIUM IN ACCESSORY MINERALS

The distribution of uranium within individual crystals was studied with the help of fission-tracks from the thermal neutron-induced fission of U-235 (in uranium-containing minerals) recorded on Lexan plastic sheets.

A total number of 111 measurements were made on fission-track radiographs of crystals during the present investigations. Uranium concentrations were measured in 28 titanite and leucoxene crystals (Tables 4.1 and 4.5), 12 allanite crystals (Table 4.6), 17 zircon crystals (Table 4.8), and 4 monazite crystals (Table 4.10).

Fission-track radiographs of 5 thin sections of gneisses and amphibolites show that almost all uranium resides in titanite, the most abundant accessory mineral. Uranium content of titanites varies from one crystal to another and ranges from 132 to 380 ppm (Table 4.5).

In fission-track radiographs of pegmatites, 80% of the tracks-covered area coincides with accessory minerals like titanite , leucoxene, allanite, zircon, cyrtolite and monazite. Nearly 15% of the tracks (by area) originate from uranothorite and uraninite grains, and the remaining 5% of the tracks are concentrated in inclusions and alterations along cracks and margins of magnetite and ilmenite grains.

Titanite: Fission-track radiographs of first generation titanite generally show a non-uniform uranium distribution across individual crystals. The distribution of tracks reveals distinct accumulation of uranium in rims of more than 60% of old titanite crystals (Plates 4.1 and 4.1R), (Table 4.1). However no differences in optical properties between

Table 4.1 Fission-track uranium determinations of titanites from mylonitized pegmatite dykes along Highway No. 648(S) near Cardiff, Ontario.

Specimen #	Crystal description	Crystal portion	U ppm
MY-A2	1. Large, fractured	Rim	731
		Core	700
MY-A3	2. Large, euhedral	Rim	832
		Core	605
MY-A4	3. Large, suhedral with bent partings	Rim	502
		Core	448
PON-A	4. Fractured, euhedral slightly altered	Rim	748
		Core	453
		Altered	581
	5. Fractured, euhedral with pressure-induced partings	Rim	771
		Core	418
		Core	369
	6. Small euhedral	Rim	747
		Core	530
	7. Fragmented crystal	Rim	614
		Core	445
PW. MG-1	8. Sub-hedral, partly altered	Altered?	531
		Altered?	568
		Clear	377
		Leucoxene	1189
		Leucoxene	1340
		Leucoxene	703
PW. MG-1	9. Highly altered rusty-brown.	Altered	883
		Altered	850
		Clear	750
		Rim	795
MY. AD	10. Small crystals replacing illmenite in fractures (second generation titanites)	Core	790
		Core	832
		Core	861
		Core	859
A-1	11. Euhedral, slightly bent	Rim	690
		Core	530
	12. small euhedral	Core	430

Table 4.2. Partial microprobe analysis of titanite (crystal No. 8 in Table 4.1) from mylonitized pegmatite (PW-MG1) along Highway No. 648(S) near Cardiff, Ontario.

No.	Element	Rim	Core
1	SiO_2	30.36	30.16
2	Fe_2O_3	2.90	3.21
3	CaO	27.32	27.33
4	TiO_2	29.24	29.22
5	ThO_2	0.09	0.10
6	UO_2	0.00	0.00
7	ZrO_2	0.00	0.00
8	Nb_2O_5	1.66	1.89
	total %	91.58	91.93

Analyst: Paul Mainwaring

Note: All iron is quoted as Fe_2O_3 and all uranium as UO_2

the marginal and central parts are observed in the titanite crystals. A large number of clustered populations of tracks are generally observed within 80% of old titanite crystals. These clusters represent radioactive inclusions within titanite (Chapter 4, art. 4.3; Plate 4.1R). Tracks are fairly uniformly distributed along uranium-rich margins and central parts of titanite crystals away from high uranium domains (radioactive inclusions).

Second generation titanites show homogeneous uranium distribution throughout the crystals. They are free of inclusions so that no clusters appear on radiographs of these titanites.

The uranium content of titanites determined by this author by fission-track counting are given in Table 4.1. Partial microprobe analysis of one titanite crystal from "A" type mylonite is given in Table 4.2. The values of U and Th reported by different authors are tabulated in Tables 4.3 and 4.4 for comparison. Various possible reasons for uranium accumulation in rims of the titanite crystals are discussed towards the end of this chapter.

Some of the titanite crystals show an increased concentration of tracks in altered parts (leucoxene?) along fractures traversing the crystals (Plates 4.2 and 4.2R). No uranium lies in these fractures where they pass through adjacent quartz and feldspar grains.

Allanite: Allanite is another abundant uranium-bearing accessory mineral in the pegmatites. Fission-track distribution is inhomogeneous in 80% of allanite crystals (Table 4.6). The yellowish-brown, narrow outer zone shows uranium enrichment as compared with the dark brown rusty core (Plates 4.3, 4.3R, 4.4 and 4.4R; Table 4.7). The allanites also contain a

Table 4.3 Uranium and Thorium content of accessory titanites from granitic rocks. (Modified after Hurley and Fairbairn, 1957, Table 3).

Sample No.	Locality	U ppm	Th ppm	Comments
3060	Mount Waldo, Maine	1270	165	gr
1971	Blueberry Mountain, Massachusetts	1380	2430	g
1970	Clayton Cone, Utah	400	560	f
1968	Idaho	370	900	e
3085	West end of Mountainville, Maine	300	1070	gr
3063	Hollingsworth and Whitney	250	375	gr
3080	Two miles N of Mt. Desrert, Route 198, Maine	245	950	gr
3071	St. Gideon, Quebec	214	40	gr
3055	Hallowell, Maine	190	140	gr
1684	Franklin, N.J.	215	190	h
1677	Lewis County, N.Y.	218	170	h
1782	Nippising, Ont.	127	70	i
3082	Six miles N of Kingston, Ont.	70	150	b
3079	One mile S of Jonesboro, Route 198, Maine	39	80	gr

b Syenite
e Gneiss
h Amphibolite
f No information
g Metasomatic rock
gr Granite
i Pegmatite

Table 4.4 Uranium and thorium contents of titanite in various rock types.

Rock description	U ppm	Th ppm	Reference
Metasediments	40-50	-	
Mafic (amphibolite)	50	-	Dostal and Capedri
Mafic (granulite)	50-88	-	(1978)
Cataclasite from albitite	140	-	Dmitriyev et al. (1979)
Unknown	10-700	-	Rich et al. (1977) Table 1, 2
Unknown	0.5-1.3	-	Yeliseyeva (1977) Table 3
Granitic rock	39-1380	40-3150	
Granitic rock	70-280	20-375	Hurley and Fairbairn
Granitic rock	105-300	20-1070	(1957)
Diorite	350	-	Ingersn (1954)

Table 4.5 Fission-track uranium determination in titanites from country rock (gneiss) along Highway 648(S) near Cardiff, Ontario.

Specimen No.	Rock Description	Crystal description	Uppm
CR.Dz	Quartz-biotite gneiss	Subrounded	250
		Subhedral	235
		Rounded	232
		Fragmented	132
PE.16	Quartz-biotite gneiss	Euhedral	270
		Subhedral	211
		Rounded	166
CR-1	Hornblende-biotite	Subhedral	271
		Same	269
		Subrounded	235
		Euhedral	257
CR-PW1	Hornblende-diopside gneiss	Euhedral	306
		Fragment	287
		Rounded	268
CR-PW2	Hornblende gneiss	Rusty-brown	380
		Euhedral	359

Table 4.6 Fission-track U determination in allanites from mylonitized pegmatite along Highway No. 648(S), near Cardiff, Ontario (sample location in Fig. 3.0).

Specimen No.	Crystal description	Crystal position	Uppm
MY-A4	1. Large, euhedral, zoned	Rusty core	1373
		Yellow rim	1675
	2. Small, euhedral, weakly zoned	Rim	1742
		Core	1340
	3. Small, euhedral, weakly zoned	Rim	1507
		Core	1340
MY-A5	4. Large, euhedral zoned	Rim	1206
		Core	1021
MY-A2	5. Large, fractured, zoned	Rusty-rim	1005
		Opaque core	921
	6. Subhedral, fractured, zoned	Rim	1825
		Core	837
		Rim	1675
		Core	860
PON-A	7. Dark-brown, fractured	Rim	1842
		Core	938
	8. Small, subhedral	Rim	1926
		Core	1038
PW-MG.1	9. Unzoned, subhedral	Rim	1297
		Core	1105
	10. Cigar-shaped, fractured	Clear core	971
		Rim	1306
		Rusty core	1026
		Rim	885
		Crack	1405
MY-AD	11. Rusty-brown	Rim	1879
		Core	1095
	12. Small, weakly zoned	Rim	1750
		Core	1158

Table 4.7 Partial microprobe analysis of allanite from mylonitized pegmatite (PW-MG1) along Highway No. 648(S), near Cardiff, Ontario (Sample location in Fig.3.0).

No.	Element	Rim 1	Rim 11	Core
1	SiO_2	32.26	29.19	30.89
2	Fe_2O_3	2.31	2.15	3.14
3	CaO	3.43	7.99	10.93
4	ThO_2	0.13	0.76	0.21
5	UO_2	0.00	0.00	0.00
6	Ce_2O_3	14.57	9.42	10.58
7	La_2O_3	9.51	6.18	9.24
8	Nd_2O_3	2.35	2.61	2.39
9	Sm_2O_3	0.26	0.43	0.37
	Total %	64.82	58.73	67.75

Rim 1: Light brown unaltered zone

Rim 11: Dark brown altered zone

Analyst: Paul Mainwaring

(Note: All iron is quoted as Fe_2O_3 and all uranium as UO_2)

number of uranium-rich domains which appear as fission-track clusters (Plates 4.4 and 4.4R). They are distinct mineral phases in allanite crystals rather than alteration products.

Allanites generally show prominent alterations. Slight increase in the uranium content was noted in altered zones by using fission-track radiographs.

Zircon: Distinctly body-zoned zircons show evenly distributed tracks throughout the crystals (Plates 4.5, 4.5R). No uranium enrichment was observed within dark bands in zoned zircons (Chapter 3). The crystalline zircons have a lower uranium content (3082 - 4793 ppm, Table 4.8) than the unzoned metamict variety (cyrtolite) (6100 - 6500 ppm,). Microscopic inclusions within metamict zircons appear as tiny clusters of fission-tracks throughout the crystals. Some of these clusters are hardly distinguishable from other tracks, therefore chances are great that the measured values may represent a mixture of uranium present in the crystal structure and contained in inclusions of submicroscopic dimension in the zircons. These inclusions were isotropic (metamict) and too fine-grained for identification by X-ray diffraction or optical microscope.

Fission-track radiographs of the rim-zoned variety of zircon reveal a distinct uranium enrichment in their rims The uranium-rich rims are zoned and often incompletely developed. They are comparable with earlier described body-zoned zircons (Table 4.8) whereas uranium concentrations in their cores are variable (2300 - 4350 ppm U). About 5% of rim-zoned zircons show fairly evenly distributed uranium throughout the crystal.

Table 4.8 Fission-track uranium determinations of zircons from mylonitized pegmatite dykes, along Highway No. 648(S), near Cardiff, Ontario. (Sample location in Fig. 3.0).

Specimen #	Crystal description	Crystal Portion	U ppm
MY-A2	1. Semi-Isotropic	Core	3350
MY-A4	2. Euhedral, rim-zoned	Rim	4522
		Core	4355
	3. Euhedral, body-zoned	Rim	4492
		Core	4450
	4. Small, rounded	Core	4325
	5. Body-zoned	Core	4205
MY-A5	6. Euhedral metamict (cyrtolite?)	Core	6500
A-1	7. Body-zoned	Rim	4793
		Core	4568
	8. Small, rounded	Core	3980
	9. Weakly-zoned	Core	3795
PON-A	10. Rim-zoned	Rim	4922
		Core	4355
PW.MG1	11. Small, rounded isotropic (cyrtolite?)	Core	6351
	12. Small, rounded (unzoned)	Core	4125
		Core	3906
	13. Small, rounded metamict	Core	6230
		Core	6100
MY-AD	14. Clear, rounded, (weakly zoned)	Rim	3350
		Rim	3082
	15. Rim-zoned	Rim	4555
		Core	2305
	16. Fragmented, (body-zoned)	Core	4390
		Core	4420
	17. Rim-zoned	Rim	5300
		Core	4210

By microprobe techniques uranium-rich rims in the rim-zoned zircons show a chemical composition different from the unzoned uranium-poor cores (Table 4.9).

Accumulation of uranium at the margins of zircons with or without the formation of new zircons has been described by several authors (Ahrens, 1965; Veniale et al. 1968; Gulson and Krogh, 1975; Gulson and Rutishauer, 1976; Clark et al. 1979; Rimsaite, 1980).

The genesis of different varieties of zircon with a brief description of uranium enrichment in the rims of rim-zoned zircons is given towards the end of this chapter.

Monazite: Monazite generally shows a homogeneous uranium distribution throughout the crystals. No variations in U content are observed in spite of evidence of alteration in the crystals. Uranium concentrations greatly differ from one grain to another (2361 ppm to 3182 ppm U) (Table 4.10).

Opaque minerals like magnetite and ilmenite occasionally show fission-tracks. They appear to have originated from widely distributed cracks and tiny patches (leucoxene?).

The data existing in the literature on the uranium content of titanite (Table 4.3 and 4.4) and zircon (Table 4.11, 4.12 and 4.13) are quite variable, but the values in general are comparable to those reported by this author (Tables 4.1 and 4.8).

Uranium content of individual minerals varies from rock to rock or within a single rock from one crystal to another. It also depends on whether the mineral is a minor accessory or an abundantly crystallized phase (Table 4.11 and 4.12).

Inhomogeneities of uranium content across individual crystals of

Table 4.9 Partial microprobe analysis of rim-zoned zircon (no. 17 in Table 4.8) from mylonitized pegmatite (MY.AD), along Highway No. 648(S) near Cardiff, Ontario.

No.	Element	Rim	Core
1	SiO_2	31.71	32.23
2	Fe_2O_3	0.28	0.42
3	CaO	2.90	0.93
4	TiO_2	0.01	0.00
5	ThO_2	0.05	0.12
6	UO_2	0.61	0.40
7	ZrO_2	56.82	60.78
8	Nb_2O_5	0.62	0.59
	Total %	92.79	95.67

Analyst: Paul Mainwaring

(Note: All iron is quoted as Fe_2O_3 and all uranium as UO_2).

Table 4.10 Fission-track uranium determinations of monazites from mylonitized pegmatite-dykes along Highway no. 648(S) near, Cardiff, Ontario. (Sample location in Fig. 3.0).

Specimen #	Crystal description	Crystal portion	Uppm
PON-A	1. Euhedral, slightly altered	Core	3015
		Rim	3182
	2. Clear, euhedral	Core	2680
		Core	2361
MY.AD	3. Slightly zoned	Core	2847
PW.MG:1	4. Euhedral, zoned	Core	2945

Table 4.11 Uranium and thorium contents of zircons in various rock types.

Rock Description	U ppm	Th ppm	Method*	Reference
Radioactive pegmatite (Madawaska Mine, Bancroft, Ont.)				
1. fine grained cyrtolite	6130	-	ID	Rimsaite (1980)
2. coarse grained cyrtolite. (refined)	5670	-	ID	Rimsaite (1980)
Plastically deformed albitite	530-1000	-	FT	Dmitriyev et. al. (1979)
Metamorphic rocks				
1. metasediments			NK	Dostal & Capedri (1978)
2. mafic (granulite)			NK	
Unknown	520-2580	-	NK	Yeliseyeva (1977)
Lauterbrunnen crystalline complex.				
1. metasediments	618-794	-	NK	
2. granitic rock	624-887	-	NK	Gulson & Rutishauser (1976)
3. granitic rock	945-1535	-	NK	
Ouzzal granulites (Algeria)				
1. clear zircon	3620-5820	431-0.11	NK	Lancelot et al. (1975)
2. brown zircon	2200-1100	3000 (Av)	NK	
Rapakivi granites (average of 40 specimens)	49-2326	-	FT	Gulson & Krogh (1975)

cont..

Rock description	U ppm	Th ppm	Method*	Reference
Metamorphic rocks				
1. detrital paragneiss	350-650	-	MP	Koppel and Sommerauer (1973)
2. zircons in their present day parent rocks	1100-6000	-	MP	
Pegmatite	7800-8640	-	FT	
Quartzite inclusions in pegmatite	715-852	-	FT	Grauert et al. (1974)
Country rock	156-768	-	FT	
Leucogranite (Central-Kazahkstan)	1190-10000	-	LS	Barnov and Tung (1961)
Granitic rock	312-3000	74-2100	NK	
Pegmatite	81-25200	10-7500	NK	
Granite	1030-1700	390-680	NK	Hurley and Fairbairn (1957)
	630-1700	75-475	NK	(Tables: 9a, b, c.)
	670-1325.	380-477	NK	

*MP: microprobe; FT: fission-track; LS: Luminecence; ID: Isotopic dilution; NK: Not Known.

Table 4.12 Uranium and thorium content of accessory zircons from granitic rocks. (Modified after Hurley and Fairbairn, 1957, Table 1).

No.	Locality	Quarry	U ppm	Th ppm
3004 a	Massachusetts, 3 mi WSW of Peabody	Lineham	1210	375
b			510	205
c			405	130
3005 a	0.5 mile WNW of Rockport	Flats Ledge	2765	1890
b			2270	1200
c			1320	740
3006 a	2 miles WNW of Rockport	Blood Ledge	970	550
b			630	380
3106 a	1.7 mile NNE of Milford	West	2004	915
b			2080	

Table 4.13 Uranium and thorium content of coarse grained zircons from pegmatites, (after Hurley and Fairbairn, 1957).

No.	Locality	U ppm	Th ppm
1661	Iredell County, N. Carolina	580	500
1669	Bucombe County, N. Carolina	730	1650
1659	Renfrew County, Ontario	140	10
1660	Brudenell Township, Ontario	105	50
1795	Haliburton County, Ontario	3520	1080
1800	N. Hastings County, Ontario	3550	3020
1799	N. Hastings County, Ontario	4380	3840
1801	Madawaska, Ontario	25 200	1600
1805	Haliburton, Ontario	5380	500
1797	Grattan Township, Ontario	6400	1050
1681	Leeds County, Ontario	81	93
1962	Wilberforce, Ontario (Treated)	4000	100
1958	Oklahoma (Nonmetamict)	300	675
1960	Oklahoma (Metamict)	1550	7500
1678	Hammond, New York	1570	600
1677	Lewis County, New York	800	10
2088	South Africa	1020	355
3038	Ceylon	5850	600

of titanite, zircon and allanite studied by this author are in agreement with observations of several other authors described below.

Barnov and Tung (1961) studied the irregular distribution of uranium in zircons, titanite and monazite by using autoradiographs. They described the relation between uranium content and degree of alteration of these minerals.

Veniale et al. (1968) described the petrological significance of accessory zircon in the granites from Baveno, Mount Orfano and Alzo (North Italy). They discussed the presence of significant amount of rounded, corroded, altered and cloudy (detrital origin) zircons often overgrown by an euhedral shell of magmatic zircons. They noted the deficiency in silica content of the old cores and higher content of Hf and radioactive elements in zoned rims. The core of some crystals were considered significantly older than the associated zircons. They described the formation of zoned rims by circulating solutions remobilized during the Alpine orageny.

Grauert et al. (1974) studied zircons in metaquartzite from the Italian Alps. According to them uranium was added in the zircons by absorption, without new crystal growth. However the process of absorption of U by zircon crystals is not explained.

Gulson and Krogh (1975) discussed the addition of U to zircons, with the formation of new zircon crystals. They studied uranium-rich rims in the zircon crystals and described them as overgrowths which probably formed during regional metamorphism.

Gulson and Rutishauser (1976) also observed the uranium enrichment in rims as compared with the body of the zircon crystals. They described the uranium-rich rims as new zircon growths, possibly

formed from granitic fluids (granitization) rather than recrystallization of older detrital zircons.

Clark et al. (1979) described the addition of uranium to the rims of zircon crystals. They studied zircons with distinct cores and overgrowths exhibiting uniform Zr and Hf concentrations across the crystals. The high uranium rims contained high Tl and Pb (radiogenic). These observations lead to various possibilities without any definite conclusion. High U and Pb content around the edges of the crystals indicate either 1) new crystal overgrowths (with associated uranium) or 2) uranium gain either from previously high uranium core or absorption and diffusion into the outer rim from an external source.

4.2 RADIOACTIVE MINERALS

The most common radioactive mineral in pegmatites from the map area is uranothorite. Uraninite is less common, but locally abundant in shear zones within pegmatite. Cyrtolite, a uranium-rich variety of zircon is another common mineral having considerable uranium content (up to 0.7%). No radioactive minerals were observed in the country rock.

Uranothorite. Uranothorite is a uranium-rich variety of thorite ($ThSiO_4$) (Steacy and Kaiman, 1978). Lang et al. (1962) defined uranothorite as a variety of thorite with more than 5 percent weight U. It is a non-metallic mineral characterized by its yellow color and isotropic nature under the microscope (Plates 4.6 and 7.0).

Uranothorite occurs as anhedral to rounded crystals within magnetite and ilmenite, generally enveloped by a thin band of hematite (Plate 4.6). It also occurs as inclusions inside titanite, (1.3 and 1.3R), allanite, (4.3 and 4.3R), and zircon. Qualitative

microprobe analysis of one uranothorite grain revealed the presence of lead (radiogenic?) along a fracture.

The analysis of 11 uranothorite specimens from Eastern Ontario by Robinson and Abbey (1957) indicates that the uranium content of uranothorite ranges from 1.68 to 20.73% U_3O_8 (Table 4.14). Some of these values may be in error because the specimens were contaminated along a network of microfractures (Robinson and Abbey, 1957). The values reported by this author by using microprobe techniques on 24 uranothorites from the Bancroft area of Southern Ontario range from 2.8% U_3O_8 to 25.88% U_3O_8 (Table 4.16).

Uraninite: Uraninite is a black metallic mineral (UO_2). It occurs as subhedral to anhedral grains in sheared pegmatites. Uraninite is generally enveloped by a thin band of hematite, like those on uranothorite. It also occurs as inclusions inside titanite, zircon and allanite. It is also found within altered xenocrysts of amphibole and pyroxene in the pegmatites.

The reported values on the uranium content of uraninite from Cardiff, Faraday and Monmouth areas (Robinson and Sabina, 1955) range from 62.7 to 73.0% U_3O_8 (Table 4.15).

The author was not able to determine the uranium content of uranothorite or uraninite by fission-track method because of the overlapping of tracks due to the high uranium content of these minerals. Uranothorites were analyzed for U and Th by using the microprobe technique (Table 4.16).

4.3 COMPARISON OF FISSION-TRACK AND MICROPROBE RESULTS

For a comparison of fission-track and microprobe results four polished thin sections were analyzed by microprobe. Chemical

Table 4.14 Partial analyses of uranothorites from Eastern Ontario. (Modified after Robinson and Abbey, 1957).

No.	Locality	U_3O_8 %	ThO_2 %
1	Topspar Fluorite Mines	13.94	46.78
2	Bicroft Mines	12.31	43.49
3	Roford Property, Monmouth Township	5.78	57.55
4	Fission Mines	11.32	49.08
5	Kenmac Chibougamau	11.72	51.56
6	Kenmac Chibougamau	10.83	48.29
7	Sebastopol Township	10.73	49.92
8	Silanco Property, Monmouth Township	9.00	52.42
9	Silanco Property Monmouth Township	1.68	58.98
10	Bicroft Mines	15.09	39.46
11	Rockingham Mines Brudenell Township	20.73	40.37
	Average	11.19	48.90

Table 4.15 Uranium and thorium content of uraninites and uranian thorianites. (Modified after Robinson and Sabina, 1955, Table 1).

No.	Location	U_3O_8 %	ThO_2 %
1	Cardiff; xx;7	73.0	7.7
2	Faraday; xi; 16, 17	70.0	7.7
3	Wakefield; iii;26	69.0	8.1
4	Cardiff; xi,xii;27,28	65.0	7.7
5	Cardiff; xv;6	66.7	8.5
6	Cardiff; xi,xii;27,28	64.5	9.2
7	Cardiff; xxi;9	66.7	10.0
8	Cardiff; xvii;A	62.8	13.6
9	Cardiff; xix;2	62.7	14.3
10	Cardiff; xii;29	68.0	17.0
11	Faraday; A;29	46.0	35.0
12*	Grand Calumet; vii;29	39.8	41.0
13*	Dungannon; xvi;14	40.0	46.4
14*	Huddersfield; v;21,22	36.3	49.7
15*	Huddersfield; iv;20	25.0	55.5

* Uranian thorianites

Table 4.16 Partial microprobe analyses of uranothorites from mylonitized pegmatite along Highway No. 648(S) near Cardiff, Ontario. (specimen # PW-MG1).

No.	UO_2%	ThO_2%
1	9.25	52.63
2	19.35	48.29
3	10.03	56.22
4	7.24	61.18
5	16.28	61.77
6	10.27	57.86
7	23.26	48.89
8	23.89	50.24
9	24.08	50.78
10	8.76	54.86
11	7.55	57.67
12	25.91	50.38
13	24.58	49.27
14	2.80	39.80

Analyst: Paul Mainwaring

composition of titanite, zircon, allanite and uranothorite were determined at different points across the crystals. Two of the thin sections were then irradiated to get the fission-track radiographs.

Microprobe techniques were found insensitive for determinations of low uranium concentrations (<1000 ppm) in most of the titanite and in some allanite crystals (Tables 4.2 and 4.7), whereas uranium content of these minerals could be determined by fission-track method (Tables 4.1 and 4.6).

Uranium content of zircon determined by fission-track method (Table 4.8) is in agreement with the values determined by microprobe (Table 4.9) in the same crystal (No. 17, Table 4.8).

Fission-track uranium determinations in titanite, allanite and zircon crystals revealed the presence of a number of tiny clusters (inclusions). The values reported in Tables 4.1, 4.6 and 4.8 are measured away from such clusters.

Uranium content as low as 100 ppm was measured in some cracks and inclusions within magnetite and ilmenite grains (Table 4.17) whereas no uranium was recognized during qualitative microprobe analysis of these features.

Clark et al. (1979) studied uranium distribution in zircons with the electron microprobe. They described the method as unsatisfactory because of its sensitivity limitations. According to them the fission-track method is much more sensitive and satisfactory for such studies.

The fission-track method has the disadvantage that it cannot measure high uranium values, whereas the microprobe is not limited

Table 4.17 Fission-track uranium determination in cracks and along grain boundaries in pegmatites from Highway No. 648(S) near Cardiff, Ontario. (Sample location in Fig. 3.0).

Specimen No.	Description	U ppm
MY-A1	Crack following magnetite grain-boundary	35
	Same crack (fission-track cluster)	52
	Crack following magnetite-quartz grain-boundary	31
	Same crack	51
PE-14	Crack passing through sheared quartz	16
	Crack following magnetite-quartz boundary	43
	Crack following quartz-quartz grain-boundary	18
	Same crack as above (different spot)	63

with respect to high U concentrations. The highest value of uranium measured during the present investigations was about 6500 ppm (Table 4.2).

Dmitriyev et al. (1979) gave the limitations of fission-track determination, ranging from as low as 0.1 ppb to about 10%. McCorkell (personal communications 1981) says that with a sufficiently small neutron dose the upper limit of fission-track method could be 100%, whereas the lower limit is about 10 ppb.

Uranium content as low as 0.8 ppm was measured by this author in some fused glasses of rock powders (Table 1.1).

CHAPTER 5. STRUCTURAL CONTROL OF U MINERALIZATION

In general terms, the localization of uranium deposits of endogeneous origin along lineaments or fault lines has been observed and described by several authors (Ruzicka, 1971; Beck, 1964).

Ruzicka (1971) described lineaments as favourable places for the location of mineral deposits which can be therefore used as criteria for prospecting. He discussed structural controls of uranium mineralization in Czechoslovakia and gave a review of the distribution of uranium deposits in the Bohemian Massif and along selected fault lines (Figure 5.0). An alignment of the uranium deposits can be seen along such lines.

Ruzicka (1971) defined a lineament as a thick zone or a fault line partly intruded by igneous rocks, locally geomorphologically predisposed to basins and grabens. It may be the boundary of geological complexes or units.

On a smaller scale the shear zones and fissures tectonically related to the lineament could be favourable sites for uranium concentration.

In Cardiff and Monmouth areas, most of the uranium deposits lie within the Grenville Supergroup paragneiss, amphibolites and marbles mantling the granitoid domes and batholiths. A vague alignment of the uranium deposits within these rocks can be seen in Figure 5.1. Lineaments No.4, 5, 6, 9, 10, 12, 14 and 15 on the map represent the prominent fault lines, from Hewitt's geological map (1957-1). The lineaments No. 1, 2, 3, 7, 8, 11 and 13

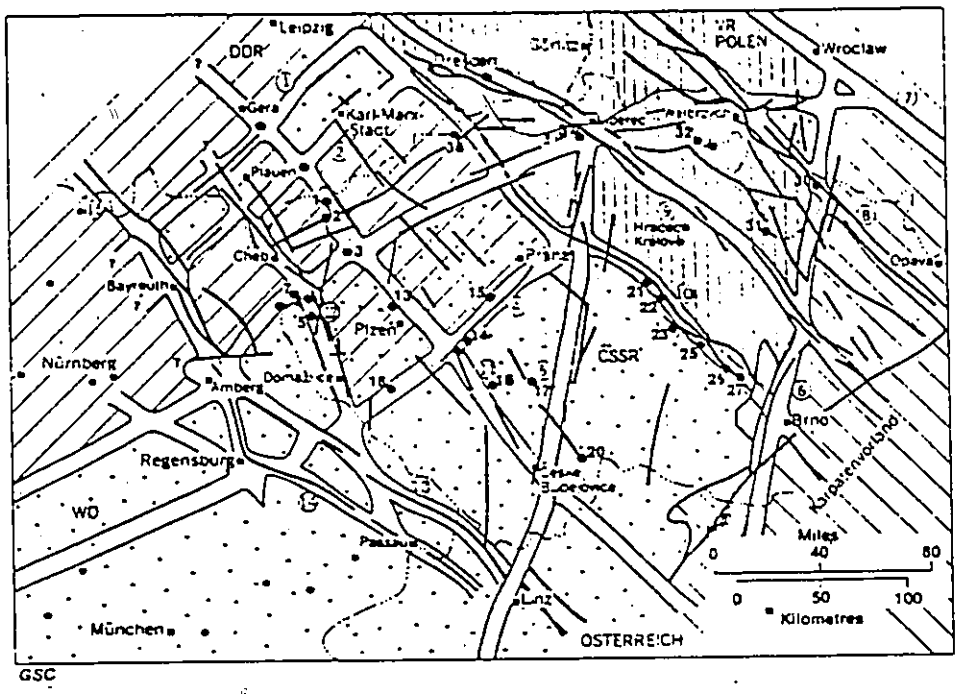

Saxony – Thuringian and Sudetic – Moravian zones

Moldanubian metallogenetic province

Lineaments . . . . . 1 / 2

Main faults . . . . . —

Bore holes . . . . . •

Uranium deposits . . . . . •26

Town . . . . . •

LINEAMENTS

1 Northeast Saxony	9 Lusatian
2 Central Saxony	10 Labe
3 Ohárec	11 Gera – České Budějovice
4 Central Bohemian (or Seam or Suture)	12 Cheb – Domažlice
5 Blanice (or Furrow)	13 Bavarian
6 Boskovice (or Furrow)	14 Danubian
7 Outer Sudetic	15 Frankian
8 Sudetic Marginal	

URANIUM DEPOSITS (Numbers refer to Figure 5)

1 Jáchymov	13 Líšany	20 O. Racouš	27 Oli
2 Hroznětín	14 Příbram	21 Bernartice	30 Jáchymk
3 Slavkov	15 Barrandien	22 Licoměřice	31 Orlické hory
4 Z. Chodov	16 Předotice	23 Čertovo	32 Žacler
5 Vítkův	17 Heřmaničky	25 Slavkovice	33 Hamr
7 Dylen	18 Dlažov	26 Rožná	35 Teplice

Fig.5.0 Distribution of uranium deposits within the Bohemian Massif in relation to lineaments and faults (after Chr et al., 1968; compiled by V. Zeitzel).

Fig. 5.1

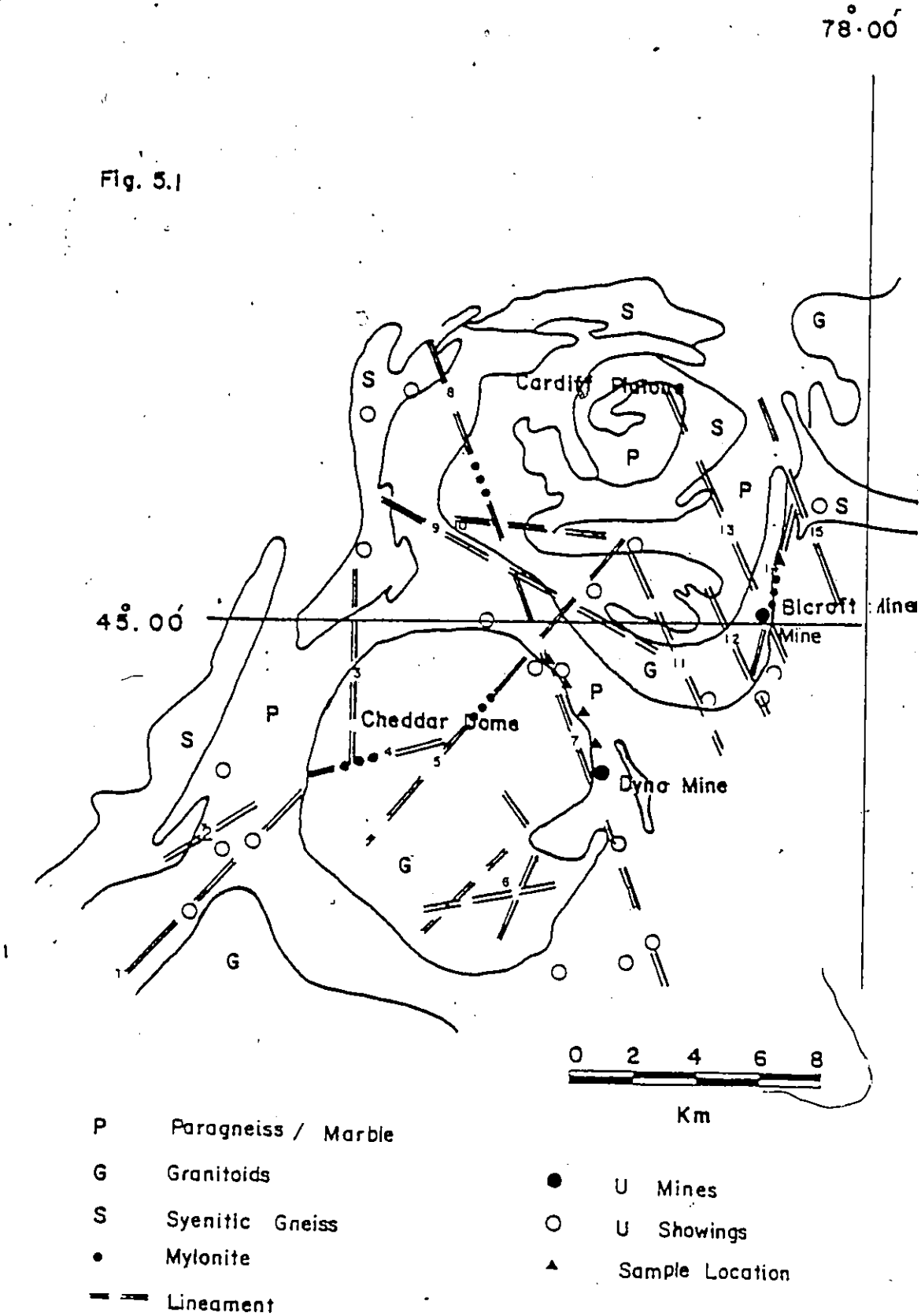

Fig. 5.1 Geological map of the Cardiff and Faraday area (after Hewitt 1957-1) showing lineaments, uranium deposits and sample locations. Lineaments No. 4, 5, 6, 9, 10, 12, 14 and 15 are from Hewitt's geological map. Lineament No. 1, 2, 3, 7, 8, 11 and 13 are added from a study of aerial photographs.

in figure 5.1 were added from a study of aerial photographs under the stereoscope. Some of these lines (1 and 7) are more hypothetical and were drawn by joining known uranium showings.

The Bicroft lineament (No. 14) was mapped on a scale of 1:15000 to determine uranium distribution as a function of distance from the lineament. The following observations were made during the mapping (Fig. 5.2):

1) Uranium concentration is mainly restricted to the pyroxene syenite pegmatite and pyroxene granite pegmatite that follow the lineament.

2) Other types of pegmatite within the lineament (leucogranitic pegmatite, syenitic pegmatite) do not show any uranium enrichment.

3) Nearly 70% of the radioactive pegmatites occur near the lineament and the remaining 30% is distributed randomly away from the lineament within rocks of the Grenville Supergroup mantling the Cardiff Pluton.

4) No prominent deformation zones were observed except one narrow B-type mylonite band (5-10 cm wide) inside one pegmatite near the lineament. No striking differences were noted in counts over the mylonitic zones and the adjacent undeformed pegmatite.

On a more detailed scale (1:1 to 1:10) the well-developed mylonite zones in pegmatites near Dyno Mine (working area "A") generally show a strong positive relationship between the uranium concentration and the shearing (Fig. 1.1).

No lineament is marked here on the geological map by Hewitt (1957-1) and no linear features were observed on aerial photographs either. Lineament "7" marked on the map (Fig. 5.1) is hypothetical and drawn by extending the fault line "8" southward.

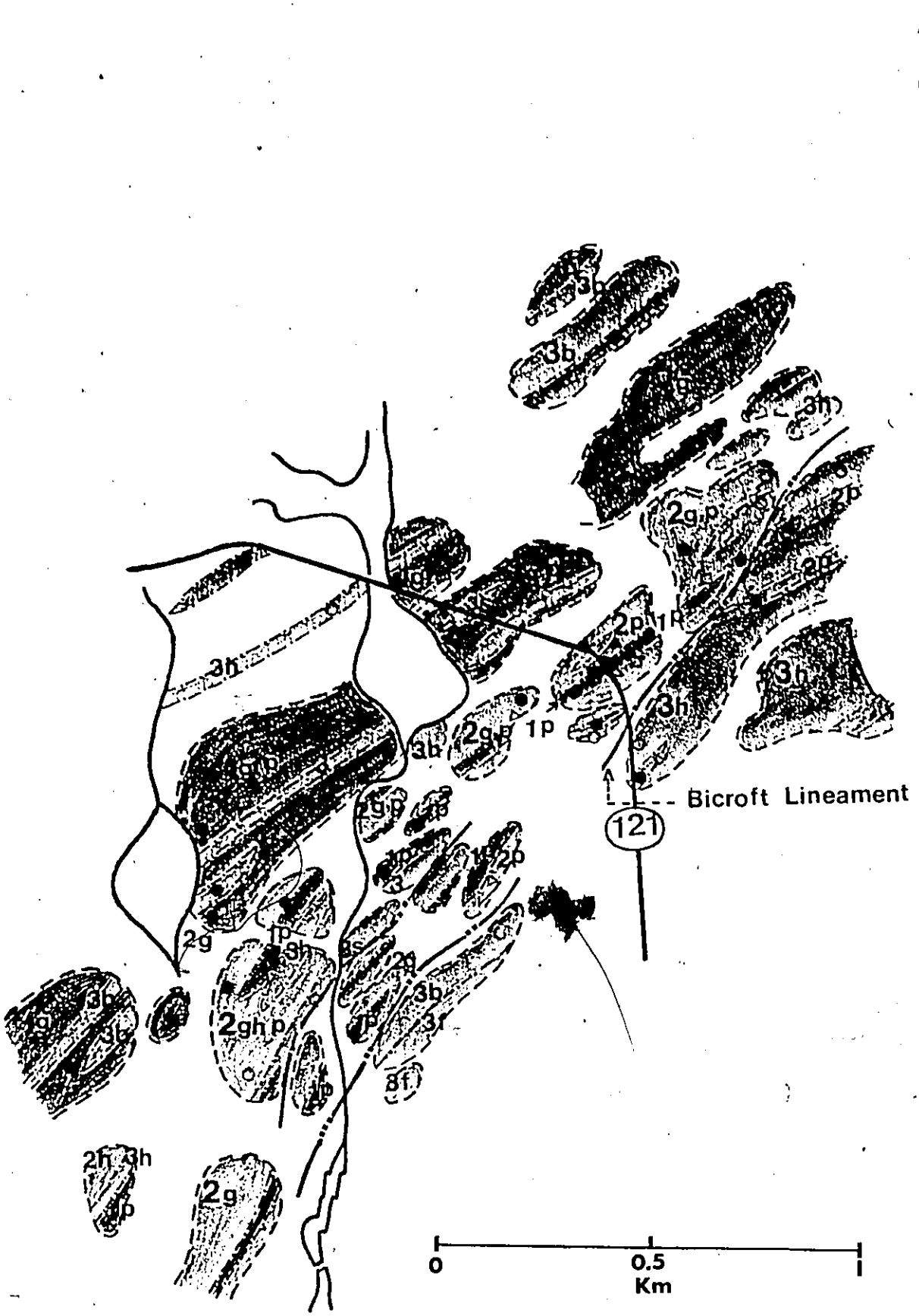
N
3b
3h
2g,p
2p
1p
3h
2p
1p
3h
3h
3h
2g p
1p
Bicroft Lineament
121
2g
3b
3f
2gh p
2h 3h
2g
0
0.5
1
Km

FIG 5.2

Fig. 5.2 Geological map of the Bicroft Lineament area.

LEGEND

Granitic rocks:

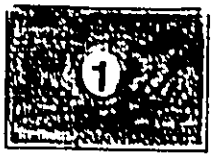

1g Granitic gneiss
1p Granitic pegmatite

Syenitic rocks:

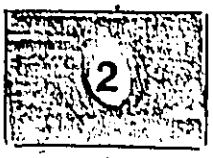

2g Syenitic gneiss
2p Syenitic pegmatite
2gh Interbanded syenite and amphhibolite

Gneissic rocks:

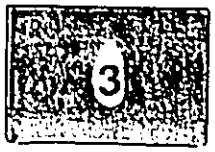

3b Quartz-biotite-plagioclase gneiss
3h Hornblende-plagioclase gneiss
3f Quartz-feldspar gneiss
3s Garnet-sillimanite gneiss,
Sillimanite gneiss

Outcrop boundary

Geological boundary

Lineaments

(CPM)

> 100	○
100 - 200	●
200 - 300	△
300 - 500	▲
500 - 1000	□
1000 - 1500	■
< 1500	■

A number of well defined lineaments occur inside the granitoid domes and batholiths (outside working area) (Fig. 5.1). The lineaments 3, 5, 8, 13 and 15 were investigated by this author during the field work of 1979. No variations in the uranium distribution were observed within and away from these lineaments, (Table 5.1) during the reconnaissance scintillation counter survey. Mylonitization (B-type) was observed in granite and pegmatitic granite within lineament "5". The scintillation counts inside and outside the mylonite do not show any systamatic variation.

Mylonitic zones in marbles of the Grenville Supergroup exposed along Monk road near the junction of Highway No. 28, nearly 4 km WSW of Bancroft were checked by scintillometer. Low counts (75-100 cpm) were recorded in marbles within and away from the mylonite zones (Table 5.1).

On the basis of field studies it appears, therefore, that no immediate connection exists between lineaments and uranium distribution. Pegmatites commonly have a higher U content than granites and gneisses. They are not restricted to the lineaments. Granites and gneisses inside a lineament do not show higher uranium concentration than rocks away from it. In most cases, a rough alignment among the uranium deposits in the area does not coincide with any visible lineament (fault line).

In contrast, a connection between the shearing and the distribution of uranium occurs on the outcrop scale. For instance, "A" type mylonites in pegmatite along Highway No. 648 (S) show a five to ten time higher radioacitivity (Figs. 1.1 and 1.1a) than B type mylonite in the same rock.

Table 5.1 Average scintillation counts (cpm) distribution across lineaments in different rock types (outside working area) near Cardiff, Ontario. (Lineaments location in F.g. 5.1).

Lineament #	Rock Description	Average Scintillation counts (cpm)	Remarks
5	1. Coarse-grained granite to granitic pegmatite (mylonitized)	120-150	Possibly within lineament.
	2. Granitic pegmatite (undeformed)	100-150	Within lineament? 4 m west of No. 1.
	3. Leucocratic granite	100-150	Within lineament? 8 m west of No. 1.
	4. Leucocratic granitic pegmatite	120-150	Outside lineament? 20 m west of No. 1.
	5. Leucocratic granite	100-120	30 m west of No. 1.
15	6. Coarse grained granite with some magnetite and titanite.	150-200	Possibly within lineament.
	7. Syenitic pegmatite	150-200	5 m east of No. 6.
	8. Leucocratic granite	100-150	10 m west of No. 6.
	9. Granitic pegmatite	120-150	20 m west of No. 6.
	10. Granitic (leucocratic)	100-120	30 m west of No. 6.
13	11. Marble (mylonitized)	75-100	Possibly within lineament along Monk Road.
	12. Marble (mylonitized)	75-80	10 m west of No. 11.
	13. Marble	75-90	50 m west of No. 11.

cont..

Lineament No.	Rock description	Average Scintillation counts (cpm)	Remarks
3	1. Pegmatitic granite granitic pegmatite (mylonitized)	120-150	Possibly within lineament.
	2. Pegmatitic granite and granitic pegmatite (undeformed)	120-150	Within lineament 4 m west of mylonitized pegmatite.
	3. Granite (leucocratic)	100-150	Within lineament? 8 m west of mylonitized pegmatite.
	4. Granite (Leucocratic)	100-150	Outside lineament 20 m west of mylonitized pegmatite.
	5. Granite (leucocratic)	100-150	Outside lineament.

5.1 MICROFABRIC AND URANIUM DISTRIBUTION

A detailed scintillation counter mapping (1:1 to 1:10) across the mylonite zone in pegmatites (outcrops No. 1 and No. 3, Fig. 1.0) suggests that radioactivity generally increases with increasing deformation, as characterized by the elongation of quartz and the kinking of feldspar and going up to complete recrystallization of quartz and in some cases ilmenite.

On the other hand no such enrichment was observed over "B" type mylonites. Both "A" and "B" type mylonites were deformed plastically and recrystallized. They are parallel to each other, striking N120°E and dipping subvertically. They may occur side by side within individual pegmatite dykes (Figs 2.1 and 2.2). From the structural point of view, they show no appreciable difference in style or intensity of deformation. Thus the "B" type mylonites do not show any uranium enrichment, although they have a microfabric similar to that of the "A" type mylonite. It does not seem that the texture is the main control of uranium distribution.

It will be shown later (Chapter 6) that the controlling factor of uranium concentration and mineralization is the petrology and geochemistry of the rock. However, the mylonites themselves are important features for the localization and concentration of uranium. They provide permeability for uranium-bearing solutions along cracks which are much more abundant in these zones than in the adjacent parts of the pegmatites.

Grain boundaries are other passages, along which solutions can move. Mylonitization involves granulation which increases the total surface area of the deformed grains, thus

providing more channels for migrating solutions.

Uranium along the mylonite fabric planes is contained within titanite, zircon, allanite, monazite, cyrtolite, uraninite and uranothorite.

CHAPTER 6 GEOCHEMISTRY

Twenty seven specimens from pegmatites and seven from the country rock (gneiss) were analyzed by X-ray fluorescence for 19 elements (Table 6.1). Pegmatites were grouped into two categories on the basis of their textural differences:
1) undeformed or slightly deformed pegmatites (13 specimens),
2) highly deformed and mylonitized pegmatites (14 specimens).

Undeformed and less deformed pegmatites were subdivided according to their radioactivity determined in the field by using scintillation-counter, into 1a) uranium-poor pegmatites (10 specimens), and 1b) uranium-rich pegmatites from uranium mines, adjacent to the working area (3 specimens).

Mylonitized pegmatites were further divided into :
2a) uranium-rich (A-type mylonites (10 specimens), and
2b) uranium-poor (B-type mylonites (4 specimens).

The silica content of country rock ranges from 47 to 56 percent, which is considerably lower than in the pegmatites (60% to 70%) in spite of their textural variations. Three uranium-rich pegmatites of group 1b show silica content slightly lower than other undeformed, uranium-poor pegmatites (1a). One sample of magnetite-rich mylonitized, highly radioactive pegmatite (PW-MG1) shows abnormally low (54%) silica content.

Sodium, calcium and magnesium do not show any systematic variation but their concentration is generally higher in country rock than in pegmatites.

Silica, potassium and iron contents of pegmatite and country rock (gneiss) reveal three distinct trends, plotted in Fig. 6.1

TABLE 6.1 Chemical analyses of pegmatites and gnelsses by X-ray fluorescence method.

Sample No.	SiO_2	Al_2O_3	Fe_2O_3	MgO	CaO	Na_2O	K_2O	TiO_2	P_2O_5	MnO	S	Ba	Cr	Zr	Sr	Rb	Zn	Cu	Ni
*																			
PE-14	76.16	13.10	0.77	0.00	0.17	3.24	6.82	0.05	0.00	0.01	0.01	386	0	146	116	347	0	100	6
PE-345	68.36	12.87	0.45	0.00	0.21	3.06	7.50	0.01	0.00	0.01	0.01	447	0	50	133	375	0	97	1
PE-78	73.54	13.42	1.80	0.13	0.35	3.60	6.59	0.09	0.00	0.01	0.02	100	0	148	101	308	0	17	6
PEG-1	75.13	14.34	1.08	0.00	1.03	5.64	2.59	0.01	0.00	0.01	0.01	124	9	62	147	113	0	0	13
PEG-2	75.18	14.45	1.06	0.00	1.03	5.81	2.61	0.01	0.00	0.00	0.01	133	0	61	144	111	0	0	0
PEG-3	71.33	13.72	1.97	0.01	0.15	3.17	7.44	0.10	0.00	0.00	0.01	385	0	100	97	374	0	0	12
PEG-5	72.66	14.03	2.00	0.04	0.15	3.31	7.56	0.10	0.00	0.03	0.01	387	5	116	102	388	7	0	10
PON-C	74.17	13.38	1.17	0.19	0.45	3.55	6.63	0.20	0.00	0.00	0.01	440	6	147	112	319	6	0	14
PON-2	70.52	15.98	0.71	0.03	0.18	3.54	9.03	0.04	0.00	0.00	0.00	510	0	23	138	408	7	0	10
PON-3	73.70	13.70	1.75	0.04	0.16	3.60	7.46	0.06	0.00	0.00	0.00	420	3	258	98	320	0	0	12
**																			
MY-A1	75.20	9.73	6.98	0.09	0.14	2.49	4.87	0.16	0.00	0.01	0.01	332	<50	394	84	243	<30	0	<40
MY-A2	74.90	9.80	6.90	0.06	0.15	2.49	4.88	0.16	0.00	0.01	0.01	335	<50	409	89	237	<30	0	<40
MY-A3	75.86	10.98	3.64	0.04	0.48	3.18	4.79	0.06	0.00	0.01	0.02	264	0	780	88	243	5	0	6
MY-A4	76.43	11.16	3.61	0.06	0.48	3.14	4.81	0.06	0.00	0.01	0.02	263	4	788	93	248	6	0	6
MY-A5	76.22	11.04	3.62	0.00	0.49	3.14	4.80	0.06	0.00	0.01	0.02	262	0	801	99	241	10	0	5
MY-AD	72.86	11.45	6.21	0.06	0.58	3.39	5.05	0.28	0.00	0.04	0.01	336	0	706	105	252	22	15	10
A-1	77.83	9.39	4.84	0.03	0.32	2.42	4.49	0.07	0.00	0.01	0.02	229	0	675	86	231	0	0	4
PON-A	73.22	11.54	5.88	0.05	0.59	3.35	5.07	0.78	0.00	0.04	0.00	329	16	621	115	245	24	0	6
PON-B	73.20	13.85	1.36	0.03	0.39	3.30	7.46	0.03	0.00	0.00	0.01	472	0	258	112	376	23	0	7
PW-MG1	54.12	6.36	30.83	0.02	0.88	0.15	3.69	1.30	0.05	0.17	0.01	248	15	2974	83	180	170	0	0
***																			
BIC	60.25	12.62	6.51	2.64	7.22	4.21	5.46	0.10	0.37	0.13	0.04	493	0	110	251	268	2307	0	6
ALP	67.79	12.37	4.90	1.07	2.88	3.40	5.30	0.04	0.01	0.18	0.00	238	1	91	86	290	432	34	0
DYNO	76.96	9.55	1.58	0.00	4.51	3.63	2.44	3.51	0.03	0.03	0.00	219	0	111	96	164	0	25	15
****																			
MY-B1	76.96	12.87	0.53	0.06	0.55	0.04	3.15	0.05	0.00	0.00	0.02	235	6	750	129	138	0	0	15
MY-B2	71.55	14.07	1.11	0.13	0.83	3.72	6.77	0.06	0.00	0.01	0.13	799	0	129	253	357	0	0	13
MY-B3	78.57	11.68	1.17	0.11	0.14	4.52	2.85	0.10	0.00	0.00	0.03	238	22	928	126	135	33	0	13
PON-1	77.96	11.67	1.11	0.11	0.39	4.71	2.82	0.10	0.00	0.00	0.03	245	14	912	115	140	47	0	13
*****																			
CR-PW1	55.60	12.83	7.38	4.08	12.47	5.02	0.46	0.73	0.21	0.21	0.01	93	37	171	184	<15	107	0	18
CR-PW2	55.27	12.76	7.41	4.04	12.65	5.04	0.46	0.78	0.24	0.20	0.01	90	26	173	201	<15	101	0	13
CR-PW3	55.99	12.86	7.42	4.12	12.78	4.98	0.92	0.79	0.19	0.21	0.01	93	49	166	191	<15	105	0	17
CR-DZ	53.85	14.07	9.94	4.65	7.21	4.77	2.13	1.55	0.30	0.19	0.07	860	115	162	577	165	35	0	66
PE-1	47.41	15.31	13.41	7.35	8.42	3.81	2.40	1.11	0.29	0.23	0.02	250	88	91	206	222	2694	0	47
PE-16	51.48	18.53	13.53	1.02	5.11	6.70	1.23	1.08	0.31	0.11	0.01	245	0	1248	398	53	897	36	0
CR-1	47.29	15.52	12.45	5.77	10.10	4.23	1.32	2.09	0.20	0.21	0.02	142	285	110	235	33	2136	19	55

* Undeformed uranium—poor pegmatites
** Mylonitized pegmatites (A-type)
*** Undeformed uranium—rich pegmatite
**** Mylonitized pegmatite (B-type)
***** Country rock

In this plot all uranium-rich pegmatites (except DYNO) roughly fall together regardless of their textural differences. They include all A-type mylonites and two of the three specimens of undeformed, uranium-rich pegmatites. On the other hand uranium-poor pegmatites in spite of their textural differences fall together in a broad field. They include all B-type mylonites and undeformed uranium-poor pegmatites.

The pegmatites in general show a wide range of SiO_2/Fe_2O_3 ratio (10 to 83) (total iron as Fe_2O_3) which suggests that they may contain any amounts of magnetite. Sheared pegmatites also show great differences between SiO_2/Fe_2O_3 ratios of uranium-rich (A-type) and uranium-poor (B-type) mylonitized pegmatites (Fig. 6.1). This indicates that any type of pegmatite may be sheared regardless of their Fe_2O_3 content and therefore then there is no necessary relationship between shearing and magnetite content.

The most striking feature of Figure 6.1 is that only the pegmatites having SiO_2/Fe_2O_3 ratio less than 20 are uranium-rich (except Dyno and PON-B).

The above observation is therefore a chemical proof of the textural interpretations and an easy way to know from chemical analysis if U is present without determining it.

Titanium and zirconium contents do not show direct relationships with uranium. High titanium and zirconium contents are found in titanite and ilmenite-rich and zircon-rich rocks. These rocks are not necessarily rich in uranium.

The radioactive, undeformed pegmatites (No.1, Fig. 6.2) carry 50 to 258 ppm Zr. On the other hand most of the mylonites

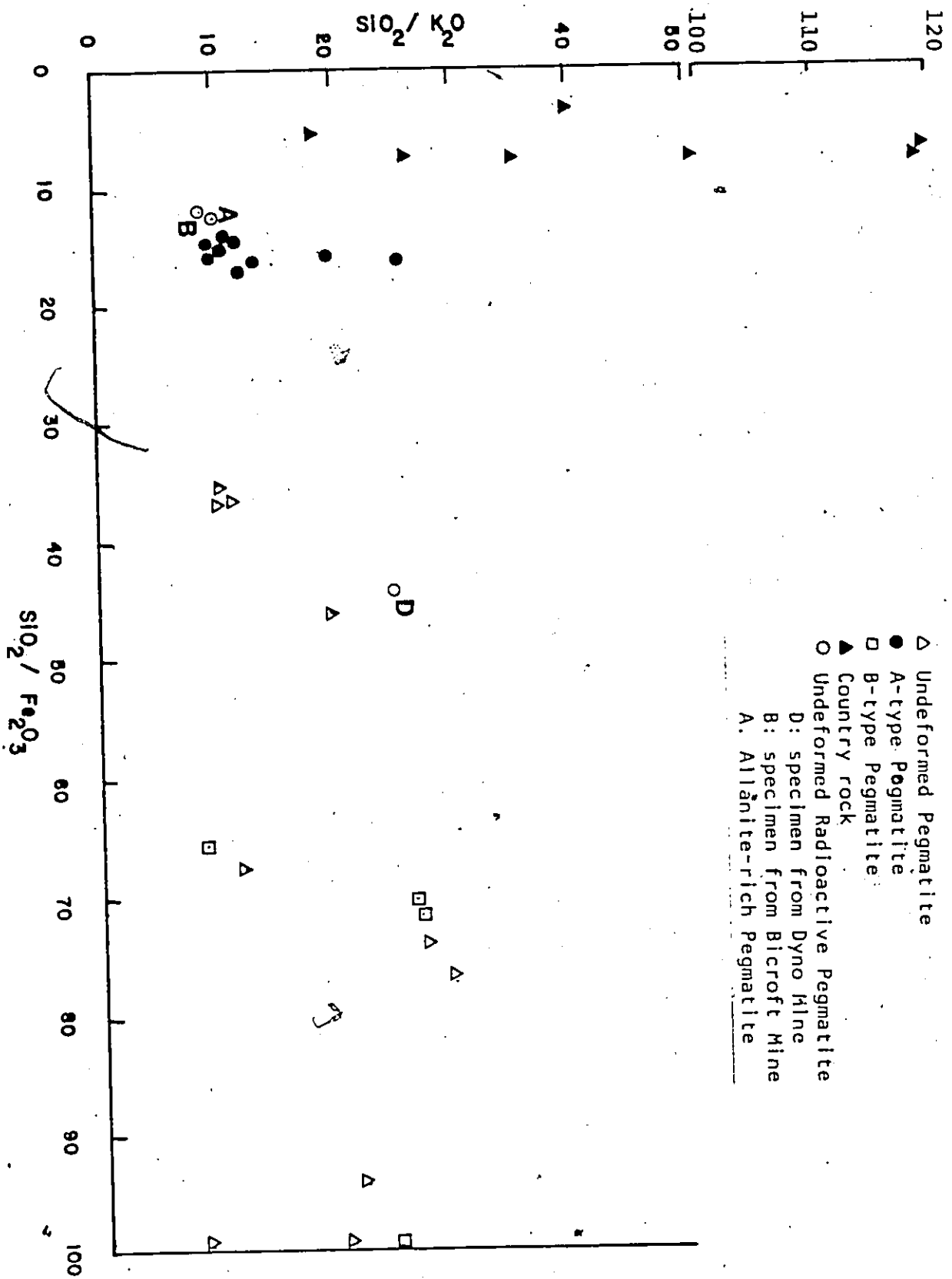

FIG. 6.1 SiO2 / K2O versus SiO2 / Fe2O3 ratios for 33 specimens from the study area (specimen # PW_MG1 not plotted).

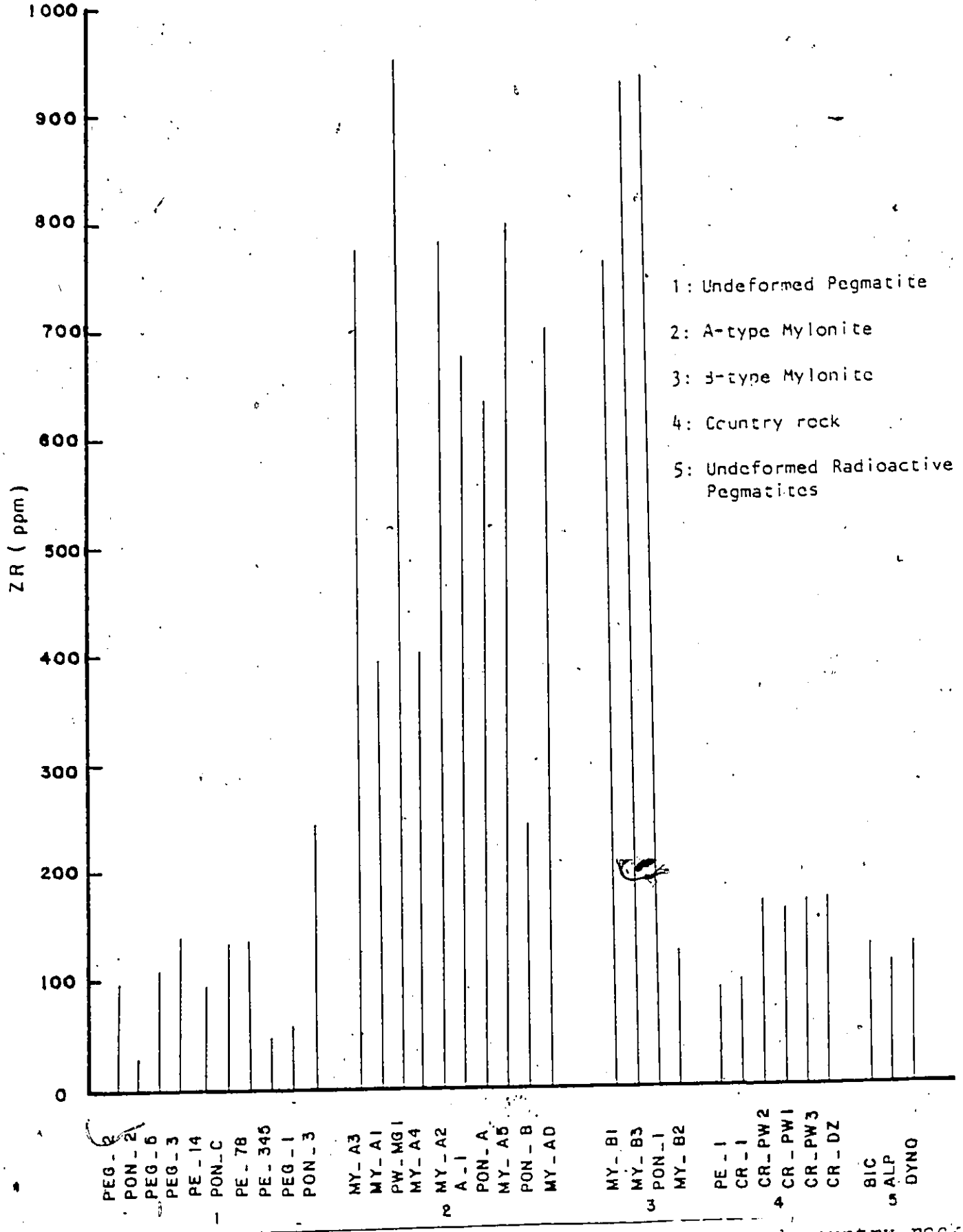

FIG. 6.2 Zirconium content in the pegmatites and country rock.

(A and B types) contain 258 to 928 ppm Zr (except MY-B2) (No. 2 and 3 in Fig. 6.2). One specimen (PW. MG1) of A-type mylonite carries up to 2974 ppm Zr (not plotted in Fig. 6.2).

Country rock (gneiss) generally show values ranging from 91 to 173 ppm Zr (No. 4 in Fig. 6.2), except one specimen (PE-16) which carries 1243 ppm Zr (not plotted in Fig. 6.2).

Higher zirconium content of mylonitized pegmatites (A and B types) as compared to undeformed pegmatites agrees with the crystallization of new zircon during or after deformation was accompanied by introduction of more Zr into the shear zones. However, the high uranium content of A-type mylonites as compared to B-type mylonites suggests that zircons are not the only important sites for uranium.

K/Rb ratios are roughly constant in all pegmatites and do not show any systematic variations with changing texture or uranium content.

CHAPTER 7. SUMMARY AND CONCLUSIONS

In Bancroft area, the importance of shearing in uranium mineralization was discussed by various authors (Ruzicka, 1971); Gordon et al.,(1978). Masson and Gordon (1979) noted that "with few exceptions, stratigraphy places only a broad geochemical control on uranium mineralization, and that structure and lithology are much more important controls".

During the present investigation the microstructural similarities between uranium-rich and uranium-poor mylonites and differences of chemical composition between the two types suggested that geochemical control is as important as structural control in uranium mineralization in the Bancroft area.

Petrographic studies and scintillation counts distribution mapping and fission-track measurements indicate that uranium is accumulated along A-type mylonite zone as compared to adjacent undeformed pegmatite.

On the basis of microstructural evidence and studies of fission-track radiographs, two generations of titanite, zircon and allanite are identified in mylonitized pegmatites.

Old titanite, allanite and zircon show a concordant relationship with mylonite-fabric. Old titanite crystals often show pressure-induced twinning and bending of parting planes (Plate 3.7) indicative of its pre-shearing origin. New titanite crystals do not show such features, they formed after magnetite

and ilmenite in A-type mylonite. New zircons are often incompletely developed and truncated (Plate 3.11). The low degree of crystallinity is possibly indicative of their formation during the process of deformation.

Studies of polished thin-sections indicate the recrystallization of ilmenite associated in magnetite stringers (Plate 3.4). The concordance of magnetite and ilmenite stringers with deformed quartz veins suggests that the origin of magnetite and ilmenite is pre-shearing or very early in the deformation process.

Old allanite and zircon crystals bear a concordant relationship with mylonite fabric which is indicative of their pre-shearing origin. New zircon formed either as separate crystals or as zoned overgrowths over old cores (Plate 3.11). New allanite crystals grow over old crystals.

Both new zircon and allanite show a uranium-enrichment by their fission-track radiographs. Partial microprobe analysis of allanite and zircon crystals show that their rims (new crystals) have a chemical composition different from their cores (Tables 4.7 and 4.9).

These observations suggest that crystallization of new grains in radioactive mylonites was accompanied by addition of uranium.

Uranium-enrichment along margins of old titanite crystals is possibly caused by the presence of microscopic radioactive inclusions. This author was able to recognize the presence of some metamict inclusions along the margins of old titanite crystals on

the basis of fission-track clusters present among less dense, evenly distributed tracks (Plate 1.5).

Larger euhedral inclusions of uraninite and uranothorite are found within magnetite, old titanite, zircon and allanite crystals (Plates 4.1 and 4.3) and in cracks preferably along mylonite fabric (Plates 7.0 and 7.0R).

The origin of pegmatites and source of uranium in the Bancroft area is a controversial topic. This author favors the model of Fowler and Doig (1979). They found an age of 970 Ma (Rb-Sr whole rock) for a radioactive pegmatite from Dyno, Greyhawk and Bicroft Mines. This age is approximately 100 Ma younger than Pb/U; Pb/Th and K/Ar ages reported by Robinson (1960) for radioactive and rock forming minerals from pegmatites. Fowler and Doig (1979) also reported an age of 1200 Ma (Rb-Sr whole rock) of the adjacent Cheddar Pluton. On the basis of low initial Sr 87/86 ratio, Doig (Personal Communication, 1980) suggested a deep-seated origin for the radioactive pegmatites, distinct from that of Cheddar Pluton.

The age of the pegmatites described by Fowler and Doig (1979) (970Ma) would be the maximum age of uranium mineralization. This author does not have geochronological evidence of the post-pegmatite uranium mineralization, but on the basis of textural studies, there was probably some time gap between the emplacement of pegmatites and the post-shearing mineralization.

On the basis of these observations the following sequence of events is proposed:

1) Emplacement of pegmatites (970 Ma). Their uranium content is quite variable. Magnetite content varies from 5 to 15% and in some cases up to 50% (PW.MG.1). Uranium is present at least in part in accessory minerals.

2) Deformation leading to formation of shear-zones and mylonites in pegmatites. Recrystallization of quartz and magnetite does not keep pace with deformation. Grain size decreases in shear-zones, so that total surface area increases.

3) Towards the end of deformation, second generation titanite, allanite and zircon crystals formed, accompanied by the introduction of uranium-bearing solutions. The formation of uraninite and uranothorite took place as incusions within magnetite and ilmenite stringers, along fractures and within first generation titanite, zircon and allanite during the last stage of deformation.

4) Crystallization of uranothorite and uraninite preferentially occurred in magnetite bands or at grain boundaries between magnetite and quartz. Fixation of uranium in these zones caused the oxidation of magnetite grains adjacent to uranium minerals.

This author disagrees with the ideas of Masson and Gordon (1979), who proposed a uranium enrichment in pegmatites during the early stages of deformation, along deformation zones within the crystallized and crystallizing pegmatite. According to them, deformation took place before

completion of crystallization. Present work clearly indicates the presence of pre-deformation and post-deformation minerals. Mylonite zones cutting pegmatites show a style of deformation that suggests that the deformation occurred after cooling of the pegmatite. Hematitization of deformed magnetite and the presence of post-deformation inclusions of uranothorite uraninite in pre-existing accessory minerals suggest that uranium was introduced into pegmatites during and after mylonitization.

REFERENCES

Adams, A.E. and Barlow, F.E.
1910 : Geology of the Haliburton and Bancroft areas; Can. Dept. Mines, Geol. Surv. Branch, Mem. 6.

Adams, J.W. and Sharp, W.M.
1970 : A convenient non-oxidizing method for metamict minerals; Amer. Min. v. 55, p. 1440-1442.

Ahrens, L.H.
1965 : Some observations on the uranium and thorium distribution in accessory zircons from granitic rocks; Geochem. Cosmochim, Acta. v. 29, p. 711-716.

Baer, A.J., Sanford, B.V. and Pool, W.H.
1970 : Gatineau River map area, NTS 31, 1:1-million; Geol. Surv. Can. map 1334-A.

Barnov, V.I. and Tung, Lieh-t-ien.
1961 : Relation between the concentration of uranium in zircon, monazite and sphene of the granites and the degree of alteration of these minerals; Geochemistry no. 11, p. 1148-1150.

Beck, L.S.
1964 : The structural environment of uranium mineralization in the Athabaska region; Can. Mining J. v. 85, p. 98-102.

Bright, E.G.
1974 : Cavendish and Anstruther Townships, Peterborough county: Summary of Field work 1974; Ont. Div. Mines, Misc. Paper 59, p. 139-145.

Bright, E.G.
1975 : Cavendish and Anstruther Townships, Peterborough county; Summary of Field work 1975; Ont. Div. Mines, Misc. Paper 63, p. 94-97.

Bright, E.G.
1976 : Cavedish and Anstruther Townships, Peterborough county; Summary of Field work 1976; Ont. Div. Mines, Misc. Paper 67, p. 122-126.

Bright, E.G.
1977 : Regional structure and stratigraphy of the Eels Lake area, Haliburton and Peterborough counties: Summary of Field work 1977; Ont. Geol. Surv. Misc. Paper 75, p. 110-117.

Bright, E.G.
1979 : The Centre Lake area, Haliburton and Hasting counties; Summary of Field work 1979: Ont. Geol. Surv. Misc. Paper 90, p. 86-88.

Clark, J.G., Gulson, B.L., Brian, L. and Cookson, J.A.
1979 : Pb, U, Hf, and Zr distributionsin zircons determined by Proton microprobe and fissuon-track techniques; Geochim. Cosmochim. Acta v. 43, p. 905-918.

Dmitriyev, V.I., Berzina, L.A. and Sannikova, L.A.
1979 : Behavior of uranium during formation of tectonites in deep fault zones; Geochemistry topics, v. 1, p. 83-85.

Dostal, J.L. and Capedri, S.
1978 : Uranium in metamorphic rock; Contrib. Mineral. Petrol. v. 66, p. 409-414.

Ellsworth, H.V.
1932 : Rare-elements minerals of Canada; Geol. Surv. Can., Econ. Geol. Ser. 11.

Fisher, D.E
1970 : Homogenized fission-track determinations of uranium in whole rock geological samples; Analytical Chemistry, v. 42, p. 50-52.

Fleischer, M.
1980 ; Glossary of mineral species; Glossary Mineralogical Record. p. 147.

Fleischer, R.L., Price, P.B. and Walker, R.M.
1975 : Nuclear Tracks in Solids. University of California Press.

Fowler, A.D. and Doig, R.
1979 : Origin of uraniferous granitoids, Grenville Province, Quebec and Ontario; Geol. Assoc. Can. Program with Abstracts, v. 4, p. 50.

Fyson, W.K., Baer, A.j., Habib, M.K. and Culshaw, N.
1979a : Structural fabric and uranium distribution in shear-zones near Cardiff, Ontario: Summary of Research, Ont. Geol. Surv. Misc. Paper 87, p. 11-12.

Fyson, W. K., Baer, A.J., Habib, M.K. and Culshaw, N.
1979b : Structural fabric and uranium distribution in shear zones near Cardiff, Ontario: Geoscience Research Seminar, Abstract, Ont. Geol. Surv.

Gordon, J,B, and Masson, S.
1978 : Uranium and thorium deposits: Summary of Field work; Ont. Geol. Surv. Misc. Paper 82, p. 181- 185.

Gordon, J.B., Colvin, A.C. and Vos, M.A.
1978 : Mineral resources studies in the Pembroke-Renfrew area, Southeastern Ontario: Summary of Field work 1978; Ont. Geol. Surv. Misc. Paper 82, p. 180-185.

Grauert, B., Seitz, M.G and Soptranova, G.
1974 : Uranium and lead gain of detrital zircons, studied by isotopic dilution and fission-track mapping;Earth and Planet. Sci. Lett. v. 21, p. 389-399.

Gulson, B.L. and Krogh, T.E.
1975 : Evidence of multiple intrusions,possible resetting of U-Pb agesand new crystallizationof zircon in the Posttectonic Intrusions(Rapakivi Granites) and gneisses from South Greenland; Geochim. Cosmochim. Acta, v.39, p. 65-82.

Gulson, B.L. and Rutishauser, H.
1976 : Granitization and U-Pb studiesof zircons in the Lauterbrunnen Crystalline Complex; Geochemical Journal v. 10, p. 13-23.

Hewitt, D.F.
1957 : Geology of Cardiff and Faraday Townships; Ont. Dept. Mines, Annual Report. v. 66.

Hewitt, D.F.
1957-1: Geological map no. 1957-1, Cardiff and Faraday Townships. Counties of Haliburton and Hastings, Ont. Dept. Mines.

Hewitt, D.F.
1967 : Uranium and thorium deposits of Southern Ontario; Ont. Dept. Mines Mineral Resources Circ. v. 4, p. 7-9.

Hurley, M.P. and Fairbairn, H.W.
1957 : Abundance and distribution of uranium and thorium in zircon, sphene, apatite and monazite in granitic rocks; Trans. Amer. Geophys. Union. v. 38, p. 934-944.

Ingerson, E.
1954 : Geochemical works of the geochemistry and petrology branch, USGS; Geochim. Cosmochim. Acta, v. 5, p. 22-39.

Koppel, V. and Sommerauer, J.
1973 : Trace elements and behavior of the uranium-lead system in inherited and newly formed zircons; Contrib. Mineral. Petrol. v.43, p. 71-82.

Kleeman, J.D. and Lovering, J.F.
1967 : Uranium distribution in rocks by fission-track registration in Lexan plastic; Science v. 156, p.512-513.

Lancelot, J., Vitrac, A. and Allegre, C.J.
1975 : Uranium and lead isotopic dating with grain by grain zircon analyses: A study of complex geological history within a single rock; Earth and Planet. Sci. Lett. v. 29, p. 357-366.

Lang, A.H.
1952 : Canadian deposits of uranium and thorium; Geol. Surv. Can., Econ. Geol. Ser. 16, first edition.

Lang, A.H., Griffith, J.W. and Steacy, H.R.
1962 : Canadian deposits of uranium and thorium; Geol. Surv. Can. Econ. Gecl. Ser. 16, Second edition.

Larsen, E.S., Jr., Waring, C.L. and Berman, J
1953 : Zoned zircons from Oklahoma; Amer. Min. v. 38, p. 1118-1125.

Little, H.W., Smith, E.E. and Barnes, F.Q.
1972 : Uranium deposits of Canada; 24th Geol. Int. Cong. Guid book for Exursion C-67.

Lumbers, S.B.
1964 : Relationship of mineral deposits in intrusive rocks and metamorphism in part of Grenville Province of Southeastern Ontario; Ont. Dept. Mines, Preliminary Report.

Lumbers, S.B.
1967 : Geology and mineral deposits of the Bancroft-Madoc area; Gelo. Assoc. Can. Guid book to Geology in parts of Eastern Ontario and Western Quebec, p. 13-30.

Masson, S. and Gordon, J.B.
1979 : Uranium mineralization and its control in immediate Bancroft area: Summary of Field work 1979; Ont. Geol. Surv. Misc. Paper 90, p. 190-191.

McCorkell, R. M.
1978 : Fission-track dating and uranium measurements. (unpublished)

NBS : NBS, brochure, certificate of analysis, Standard Reference Materials,
1970 National Bureau of Standards, U.S. Department of Commerce, Washington, D.C. 20234, August 5, 1970.

Rich, R.A., Holland, H.D. and Petersen, U.
1977 : Hydrothermal uranium deposits, Elsevier, Amsterdam.

Rimsaite, J.
1980 : Mineralogy of radioactive occurences in the Grenville Structural Province, Bancroft area, Ontario: A progress report; Current Research, Part A, Geol. Surv. Canada. Paper 80-1A, p. 253-264.

Robertson, J.A.
1977 : Uranium deposits of Ontario; Summary of Field work, 1977. Ont. Geol. Surv., Misc. Paper 75, p. 185-187.

Robinson, S.C. and Abbey, S.
1957 : Uranothorite from Eastern Ontario: Can. Min. v. 6, p. 1-14.

Robinson, S.C. and Hewitt, D.F.
1958 : Uranium deposits of Ontario; second United Nations internat. Conf. on the peaceful use of Atomic Energy, Geneva. p. 498-501.

Robinson, S.C. and Sabina, A.P.
1955 : Uraninite and thorianite from Ontario and Quebec; Amer. Miner. v. 40, p. 624-633.

Robinson, S.C.
1960 : Notes on the interpretation of U-Pb, Th-Pb and K-Ar ages in the Bancroft Ontario region. Geol. Surv. Canada, Paper 60-17, p. 41.

Ruzicka, V., ed.
1971 : Geological comparison between East European and Canadian Uranium Deposits; Geol. Surv. Canada, Paper 70-48, p. 196.

Satterly, J.
1955 : Radioactive mineral occurences in the Bancroft area; Ont. Dept. Mines, Annual Report 65, p. 6.

Steacy, H.R. and Kaiman, S.
1978 : Uranium minerals in Canada, their description, identificatin and field guides. In MAC Short course, v. 3, ed. M.M. Kimberley, p. 107-125.

Veniale, B., Pigorini, Band Soggetti, F.
1968 : Petrological significance of the Accessory Zircon in the granites from Baveno, M. Orfano and Alzo (N. Italy); 23rd Int. Geol. Cong. (Prague) v. 13, p. 243-268.

Yeliseyeva, O.P.
1977 : Uranium in granitiod accessory minerals; Geochemistry International, v. 73, p. 46-48.

Plate 1.0 Contact between pegmatite dyke and quartz-biotite gneiss. A mylonite zone runs parallel to the margin of the dyke. (Outcrop No. 4 in Figure 3.0)

Plate 1.1 Pegmatite dyke cutting quartz-biotite gneiss. Several mylonite zones run parallel to the margin of the dyke. Drill holes show the sampling technique. (Outcrop No. 4 in Figure 3.0)

Plate 1.0

Plate 1.1

PLATE 1.2 Etched fission-tracks (X 150, parallel nicols).
(Photograph donated by Dr. McCorkell).

PLATE 1.2

Fission-tracks (X 150)

PLATE 1.3 Photomicrograph of a pegmatite (specimen # MY-A3). Allanite crystal showing a dark brown (semi-opaque) core and light brown marginal zone(new crystal ?). (X 20, crossed nicols).

PLATE 1.3R Photomicrograph of the fission-track radiograph of the above specimen. High uranium concentration is in uranothorite (U) and low uranium is in accessory minerals (titanite:T and allanite:A). Dark spots (Fission-track clusters) within accessory minerals indicate the presence of radioactive inclusions in the crystals. (X 20, parallel nicols).

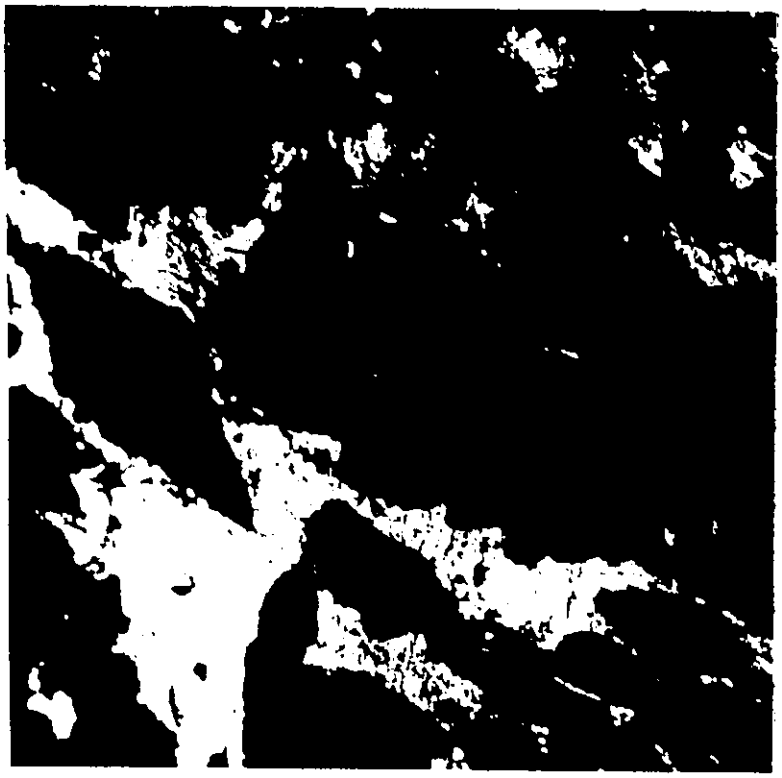

PLATE 1.3

PLATE 1.3R

PLATE 1.4 Photomicrograph of a Lexan overlay (Fission-track radiograph) (specimen # MY-A2). Uranium distribution within individual crystals can be seen. (X 5, parallel nicols).

PLATE 1.5 Photomicrograph of a single titanite crystal from the above specimen. Uranium accumulation along margin and cracks is visible. Several fission-track clusters which represent tiny radioactive inclusions are randomly distributed. U: Uraninite (parallel nicols, X 50).

PLATE 1.4

PLATE 1.5.

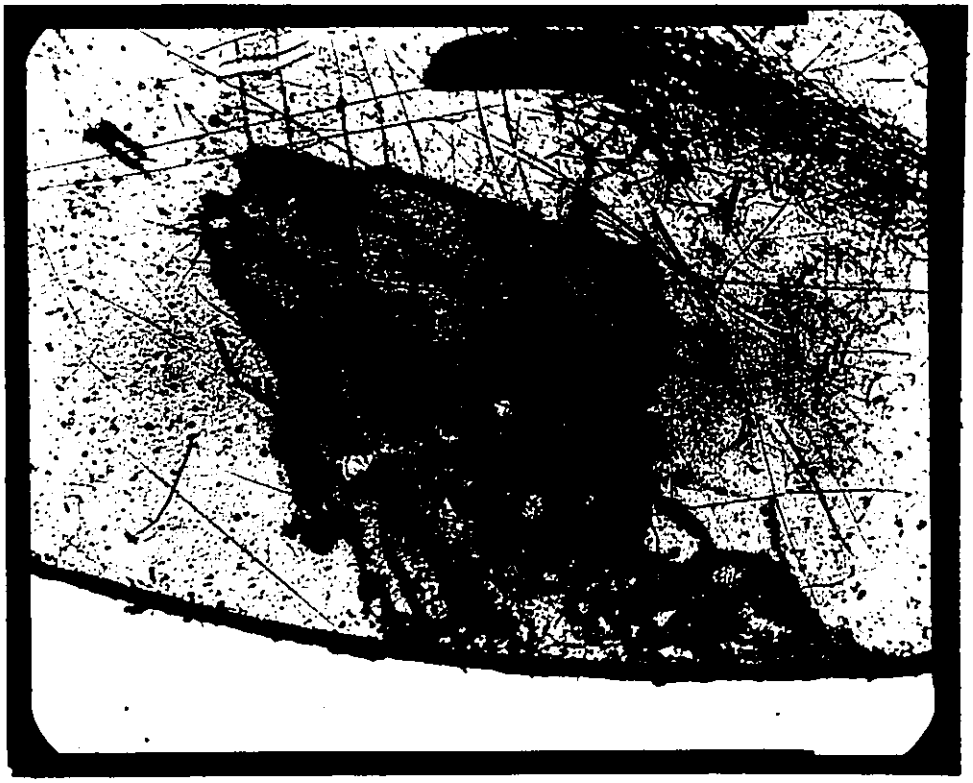

PLATE 2.0 Contact between a pegmatite dyke and quartz-biotite gneiss along Highway No.648 (S) near Cardiff, Ontario.

PLATE 2.1 A narrow pegmatite dyke cutting gneiss, along Highway No. 648 (S) near Cardiff, Ontario. Pegmatite shows abnormally high amount of magnetite (grey), titanite and leucoxene (yellow). Both margins of dyke are mylonitized.

PLATE 2.0

PLATE 2.1

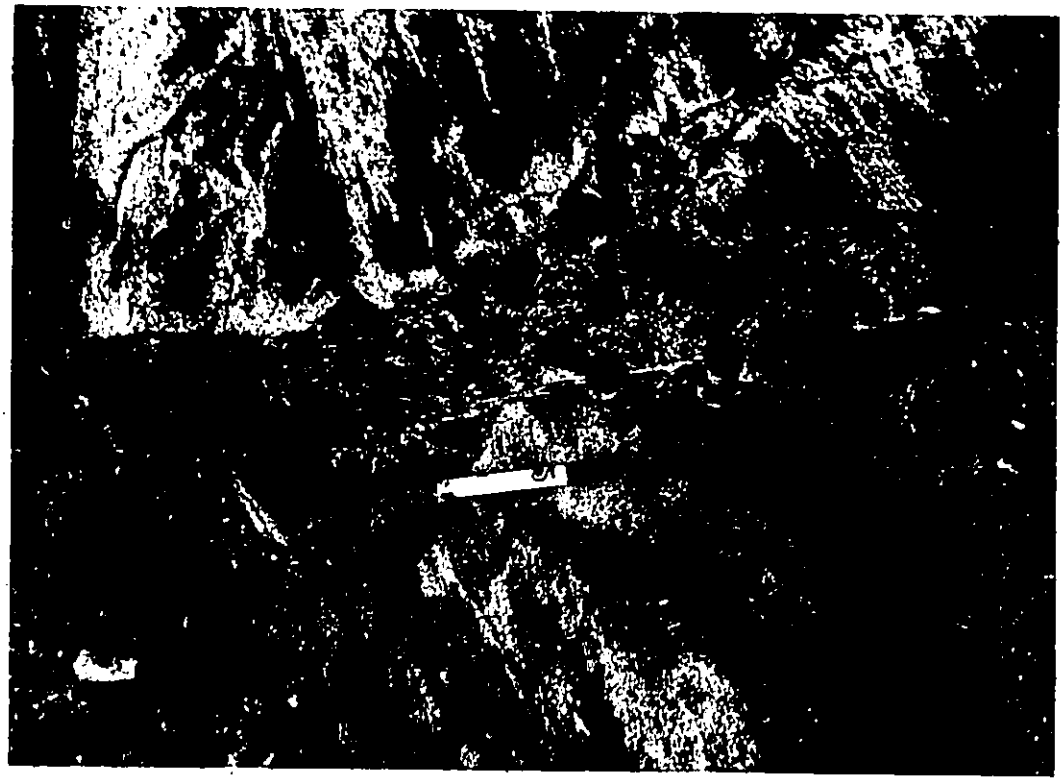

PLATE 3.1 Photomicrograph of "A" type mylonite (specimen # MY-A5). Stringers of magnetite and ilmenite (Ma) irregularly alternating with thin bands of recrystallized quartz (Q). A number of accessory minerals (circled) and few uranothorite crystals (U) are present.

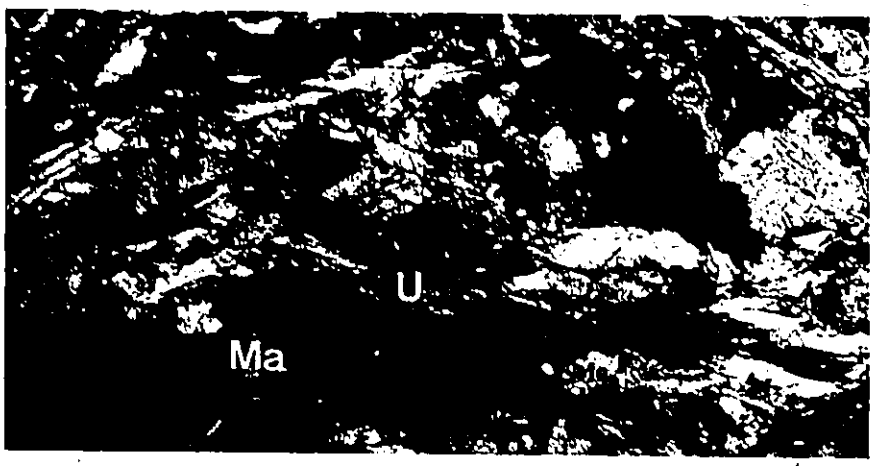

PLATE 3.1

PLATE 3.2 Photomicrograph of "B" type mylonite (specimen # MY-B2). Highly deformed and recrystallized quartz-rich (Q) bands alternating with K-feldspar (K) and hematitic plagioclase-rich bands. (crossed nicols, X 5).

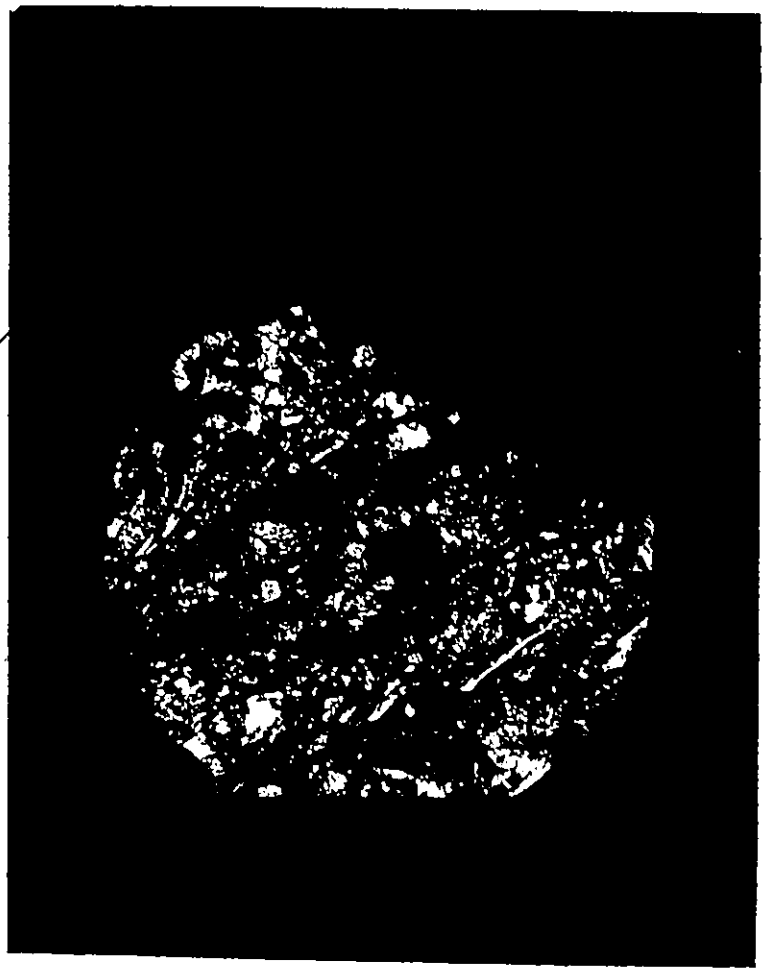

PLATE 3.2

PLATE 3.3 Photomicrograph of a mylonitic pegmatite (A-type). Large titanite (T), allanite (A) and uranothorite (U) crystals associated with magnetite (M). (X 25, crossed nicols) (specimen # PW-MG1).

PLATE 3.4 Photomicrograph of magnetite and ilmenite (polished thin section). Magnetite (M) show a number of pits and cracks. Ilmenite (I) show exsolution lamellae of hematite (H). (X 50, crossed nicols) (specimen # PW-MG1).

PLATE 3.3

PLATE 3.4

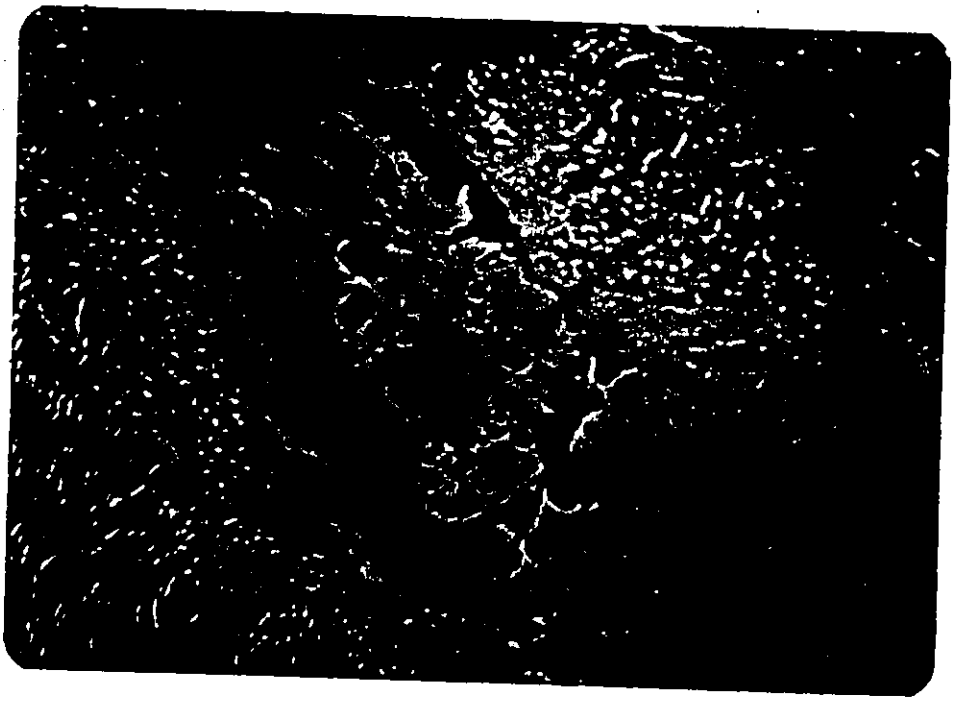

Plate 3.5 Photomicrograph of a polished thin section (PW-MG1). Magnetite (M) traversed by fractures, showing hematitization along margins at contact with titanite (T) and allanite (A) crystals. (X 25, crossed nicols).

Plate 3.6 Photomicrograph of a mylonitic pegmatite. Large monazite (M) and zircon (Z) crystals associated with bands of recrystallized quartz. (X 15, crossed nicols) (specimen No. PON-C).

Plate 3.5

Plate 3.6

PLATE 3.7 Photomicrograph of a pre-shearing titanite crystal. The crystal show distortion, and bent partings. Parting planes and fractures occupied by magnetite (M) and recrystallized quartz (Q). (X 25, crossed nicols) (specimen MY-A4).

PLATE 3.8 Photomicrograph of a large allanite crystal from mylonitic pegmatite. Coarse grained inclusions of cyrtolite (C), and uranothorite (U) are visible near the edge of the crystal . (partially crossed nicols) (specimen # PW-MG1).

PLATE 3.7

PLATE 3.8

PLATE 3.9 Photomicrograph of a mylonitic pegmatite (specimen # PW-MG1). Second generation titanite (yellowish brown) replacing magnetite and ilmenite in fractures. (X 40, crossed nicols).

PLATE 3.10 Photomicrograph of a single crystal of allanite from mylonitic pegmatite. Crystal shows a light yellow, narrow, marginal zone and an inner yellowish brown core. (X 25, crossed nicols) (specimen # PW-MG1).

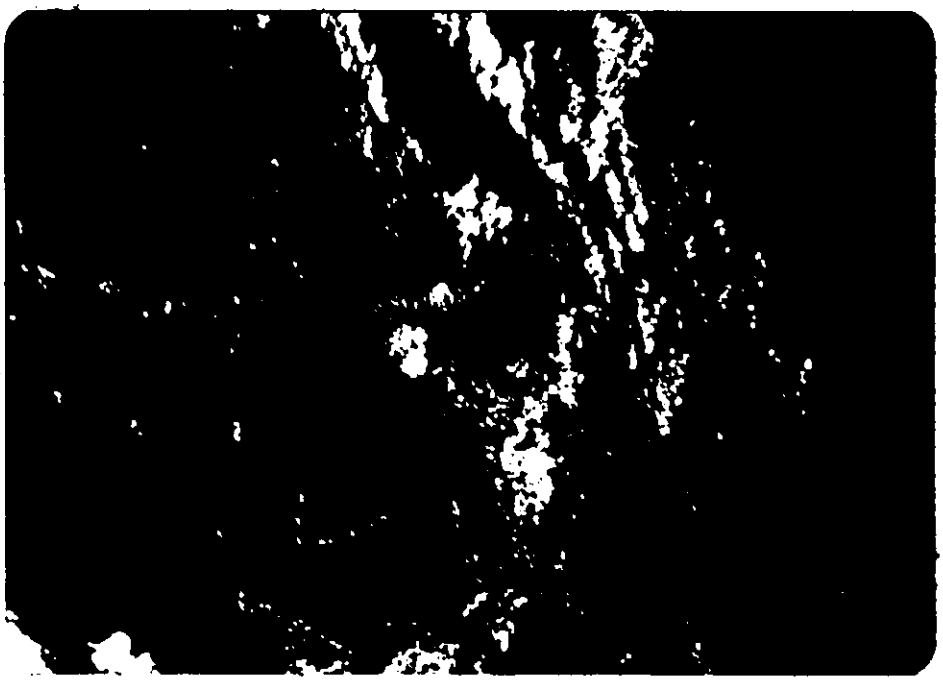

PLATE 3.9

PLATE 3.10

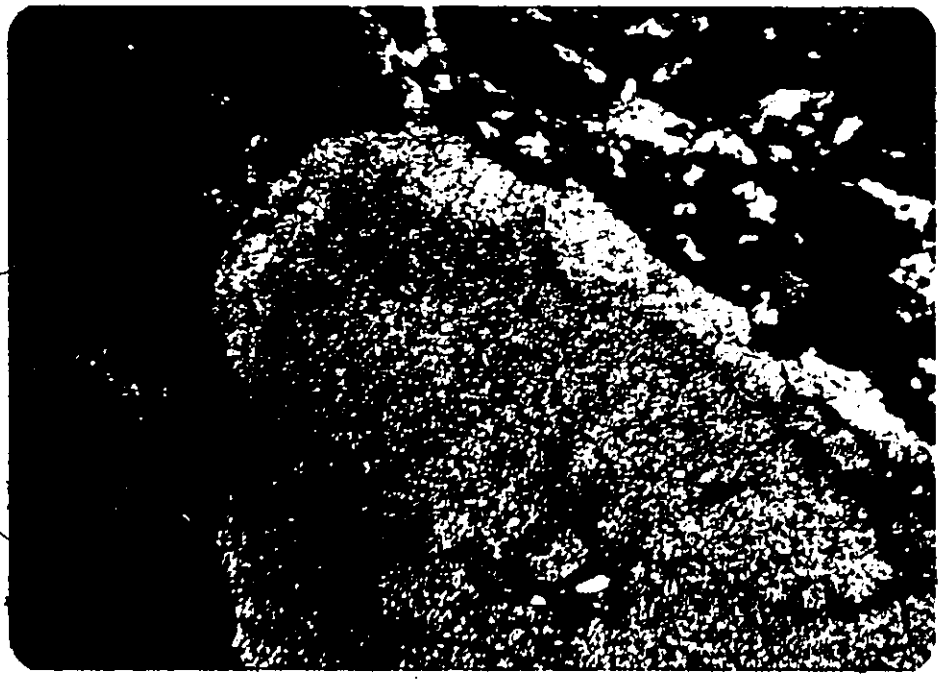

PLATE 3.11 Photomicrograph of a mylonitic pegmatite showing a distorted rim-zoned zircon crystal. The crystal is enveloped in a hematite band. (X 25, crossed-nicols) (specimen # MY-AD).

PLATE 3.11a Photomicrograph of a mylonitized pegmatite showing a rim-zoned zircon crystal with a cloudy core (old crystal ?) (specimen # MY-A2).

PLATE 3.11

PLATE 3 11a

PLATE 4.1 Photomicrograph of a pegmatite (specimen # PW-MG1) showing allanite (A), titanite (T), and uranothorite (U) crystals. A cyrtolite (C) inclusion is visible in allanite crystal. Note a concordance between these crystals and the mylonite fabric. (X25, crossed nicols).

PLATE 4.1R Microphotograph of the fission-track radiograph of above specimen. (X 25).

PLATE 4.1

PLATE 4.1R

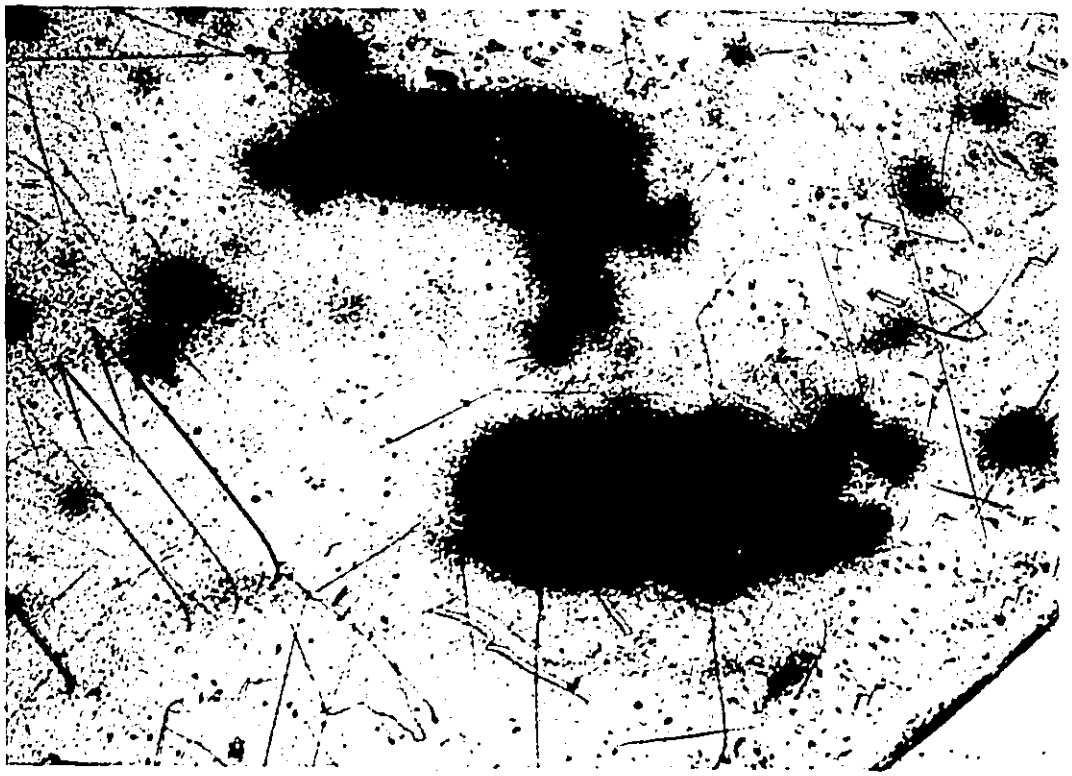

PLATE 4.2 Photomicrograph of a polished thin section. Large titanite crystals (T) showing alteration to leucoxene (L) along fractures. (X 20, crossed nicols) (specimen # PW-MG1).

PLATE 4.2R Photomicrograph of the fission-track radiograph of above thin section. Fission-track distribution showing the uranium accumulation along margins and along cracks (filled with leucoxene). (X 20, parallel nicols).

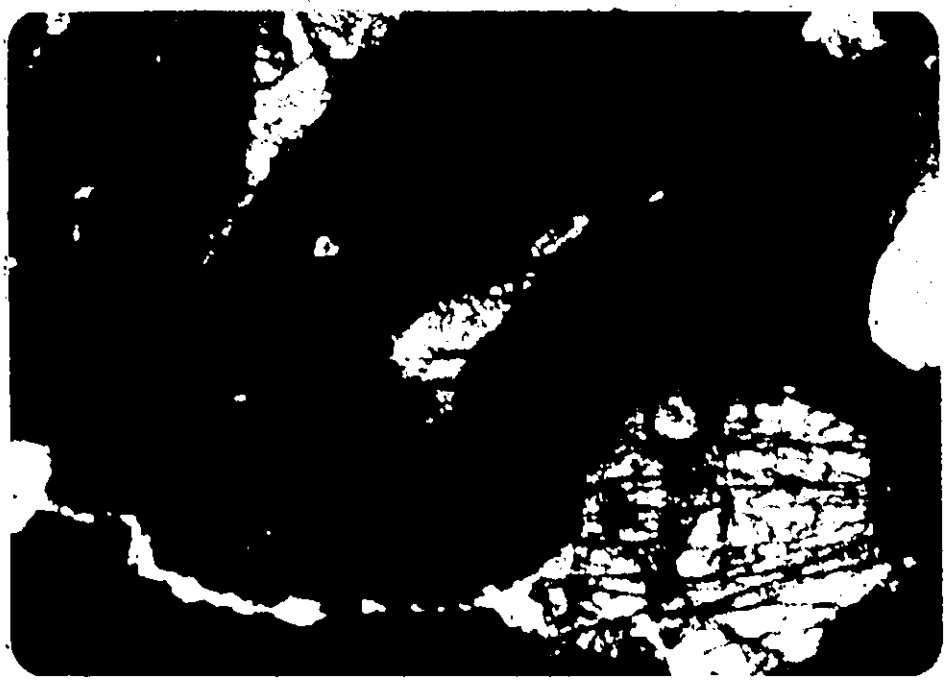

PLATE 4.2

PLATE 4.2R

PLATE 4.3 Photomicrograph of a pegmatite (specimen # MY-A2). Allanite crystals showing a narrow, discontinous zone along its margin. Note a tiny uraninite (U) crystal within allanite . (X 20, crossed nicols, specimen No. MY-A2).

PLATE 4.3R Photomicrograph of the fission-track radiograph of above specimen. Track distribution indicates uranium enrichment along margins of the allanite crystal. Fission-track clusters(dark patches) indicate the presence of radioactive inclusions. (X20, parallel nicols).

PLATE 4.3

PLATE 4.3R

PLATE 4.4 Photomicrograph of a pegmatite (specimen # MY-AD) show three large allanite crystals (A). Each crystal shows a thin, discontinous, light brown marginal zone. (X 15, crossed nicols).

PLATE 4.4R Photomicrograph of above specimen. Fission-track distribution indicates the uranium accumulation along margins of the crystal. (X 15, parallel nicols).

Note: Plate 4.4R is the mirror image of plate 4.4.

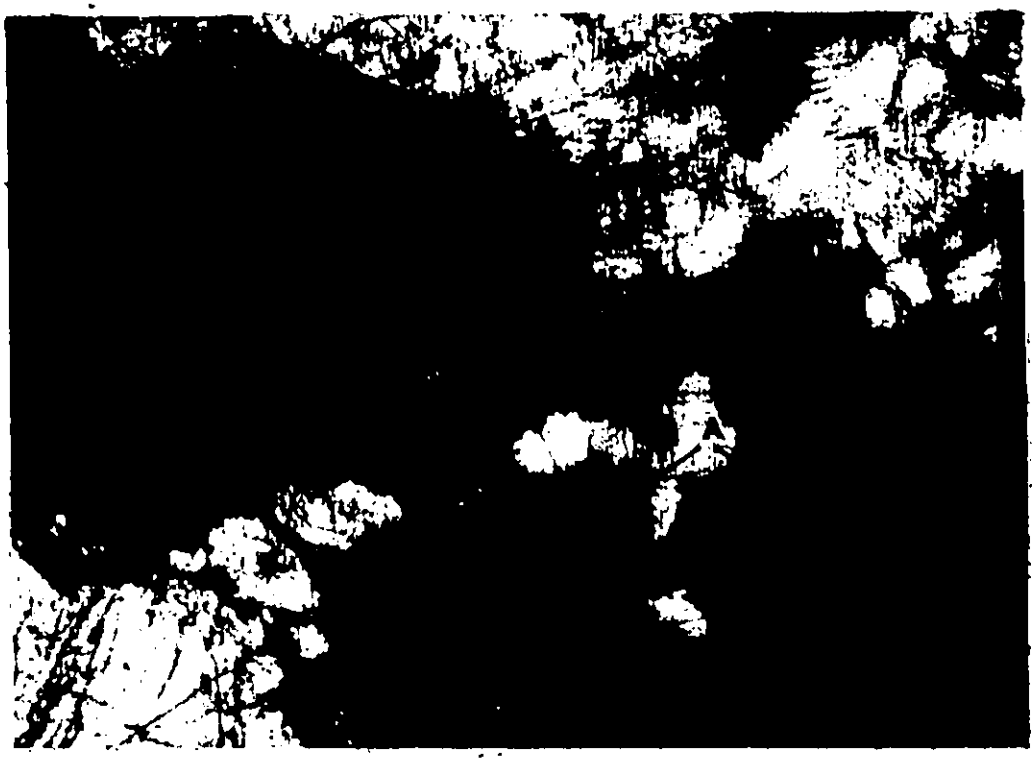

Plate 4.4

Plate 4.4R

PLATE 4.5 Photomicrograph of a mylonitic pegmatite showing a large number of rim-zoned zircons lying along the mylonite fabric. (X 15 parallel nicols) (specimen # MY-AD).

PLATE 4.5R Photomicrograph of the fission-track radiograph of the above specimen.

Plate 4.5

Plate 4.5R

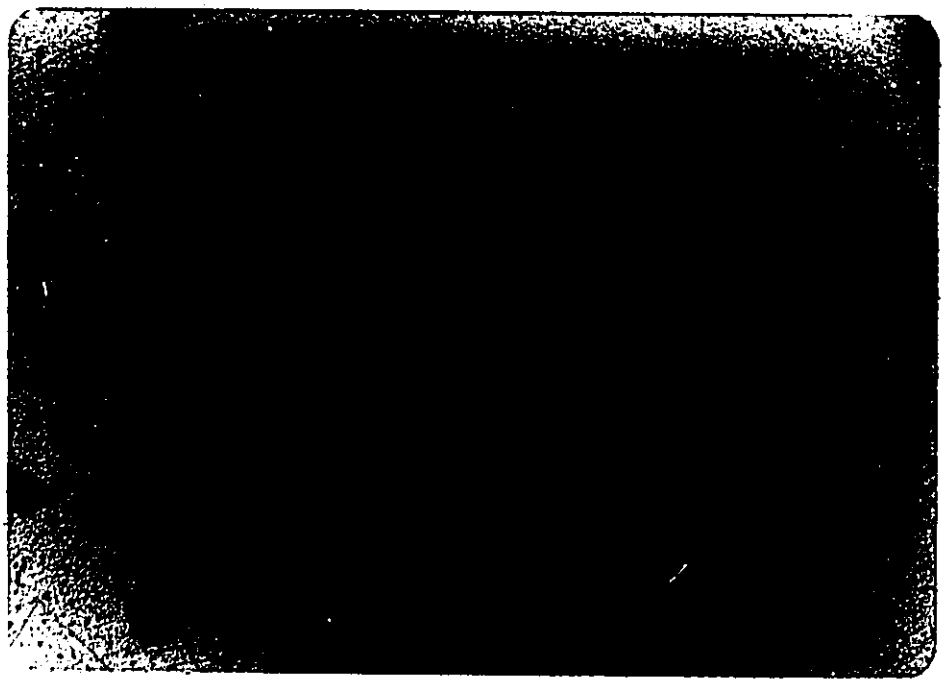

PLATE 4.6 A large uranothorite crystal (U) associated with magnetite (M). Both, uranothorite and magnetite show hematitization (H) along their margins. (specimen # PW-MG1) (X50, parallel nicols).

PLATE 4.6

Plate 7.0 Photomicrograph of a partly sheard pegmatite (specimen No. MY-A4). Uranothorite (U), cyrtolite (C), zircon (Z), allanite (A) and magnetite (M) are present in sheared parts of the pegmatite. Fractures running along and across the mylonite fabric. (X 25, crossed nicols).

Plate 7.0R Photomicrograph of the fission-track radiograph of the above specimen. Uranium is preferably present in the fractures along the mylonite fabric.

Plate 7.0

Plate 7.0R